ACS Photonics

pubs.acs.org/journal/apchd5

Perspective

Flexible and Stretchable Photonics: The Next Stretch of Opportunities

Sarah Geiger,[‖] Jérôme Michon,[‖] Siyi Liu,[‖] Jun Qin, Jimmy Ni, Juejun Hu, Tian Gu,* and Nanshu Lu*

Cite This: https://dx.doi.org/10.1021/acsphotonics.0c00983

Read Online

ACCESS | Metrics & More | Article Recommendations

ABSTRACT: Conventional electronic and photonic devices are inherently 2D and rigid because of the substrates on which they are fabricated. However, the world is not flat and stiff: There are many applications that would benefit from soft devices and nonplanar geometries, such as interfacing with the soft, curvilinear, and dynamic surfaces of living organisms. This mismatch demands flexible and stretchable devices that can be mechanically deformed (bent, folded, twisted, stretched, or compressed) without damage to their useful properties. Here we furnish an overview of state-of-the-art material, design, processing, and device technologies underlying the rapidly evolving area of flexible and stretchable photonics. We further offer our perspective on the key enabling technologies that will define new growth opportunities in this field as emerging applications of flexible and stretchable photonics continue to unfold.

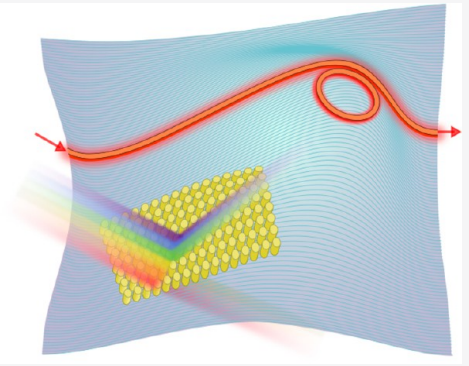

KEYWORDS: *flexible photonics, stretchable photonics, 3D fabrication, optical materials, conformal optics, metamaterials*

The successes of flexible and stretchable electronics over the past two decades have firmly established many benefits compared with their planar, rigid counterparts, including amenability to large area,[1] low-cost fabrication via roll-to-roll (R2R) processing,[2−6] as well as conformal and even imperceptible integration with biological tissues.[7−11] Thanks to novel materials, designs, and processes developed over the past decades,[12−17] numerous flexible and stretchable electrical components have been demonstrated, including metal routings, transistors, wireless transmitters, batteries, photodiodes, and light-emitting diodes (LEDs).[18−27]

Flexible photonics has emerged in an effort to provide the same deployment flexibility to optical systems. Flexible photonics, defined here as encompassing the flexible counterparts of micro- and nanophotonics (in particular, photonic integrated circuits and optical metamaterials), brings additional features to the table. Compared with electronics (which we take to include free-space optoelectronic components such as LEDs and photodiodes), it presents the advantages of allowing for an enhanced control of light propagation and light−matter interaction, which translate to light delivery with minimal loss and cross-talk. Its large multiplexing capability results in a smaller footprint for devices. It also differentiates itself from fiber optics by its enhanced geometry diversity and tight optical confinement that allows for strong light−matter interactions. Complex geometries without axial symmetry can, notably, be readily defined in the high-volume production of flexible photonics with much greater ease than in fiber optics.

This Perspective seeks to provide an overview of the burgeoning field of flexible and stretchable photonics and point to promising research directions that foresee new application opportunities. We will first succinctly review the materials, design, and processing techniques currently available for flexible photonics fabrication, followed by an overview of the applications of these devices to date. Further information on specific applications can be found in recent specific reviews on sensing,[28] metasurfaces,[29] healthcare monitoring,[30] and integration with electronics.[31] Finally, we examine the challenges limiting flexible photonics and detail several technologies that promise to both improve the performance of flexible photonics in current implementations and enable applications in new areas.

MATERIALS FOR FLEXIBLE PHOTONICS

Polymers. Polymers have long been a common material choice for flexible photonics.[32−36] The benefits of polymer waveguides include their inherent compliance, low-temperature processing, and refractive index tunability. The large degrees of freedom in C−C or Si−O bonds and the variability

Received: June 18, 2020
Revised: August 26, 2020
Accepted: September 2, 2020
Published: September 2, 2020

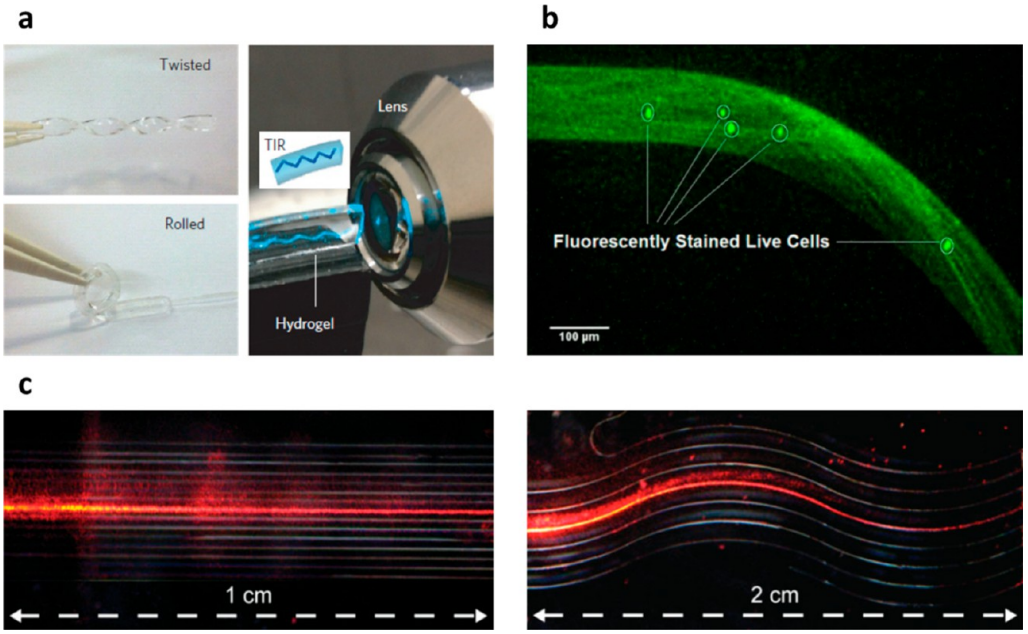

Figure 1. Waveguiding biomaterials. (a) Mechanically flexible PEG slab guides lit by total internal reflection (TIR). Reprinted with permission from ref 60. Copyright 2013 Springer Nature. (b) Stamped agarose waveguide encapsulates living breast cancer cells stained with calcein. Reprinted with permission from ref 76. Copyright 2012 Optical Society of America. (c) He:Ne laser light is edge-coupled and guided in printed silk waveguides on a glass substrate. Reprinted with permission from ref 77. Copyright 2009 Wiley-VCH.

of the degree of cross-linking allow polymers to undergo elastic deformation.[32] Polymers can bend, stretch, and conform to 3D surfaces, making them an excellent choice for R2R processing, epidermal devices, and *in vivo* applications. Moreover, compared with inorganic photonic materials, polymers are intrinsically inexpensive and compatible with low-cost processes such as printing, casting, and molding.

Photoactive acrylates or epoxies that can be bought as proprietary photoresists or adapted from known formulations are still the most popular polymeric waveguide materials because they are easily patterned using established lithography techniques and have relatively high refractive indices.[37−42] Silicones such as polydimethylsiloxane (PDMS) are also popular waveguide or substrate materials because they are easily molded, thermally stable, chemically inert, and biologically compatible and, as such, are easy to integrate with other materials.[43−49] Alternative polymers such as paralyne C and polyimides and hybrid organic−inorganic polymers such as Ormocers have also been used as flexible waveguides.[49−54]

The drawbacks of the use of polymer waveguides are their relatively low index contrast and thus the need for large waveguide dimensions, which constrain their use in photonic designs such as diffractive optical elements, photonic crystals, and metamaterials. These limitations can be overcome by hybridizing inorganic and organic materials in photonic structures to take the best of both worlds, as we shall discuss later.

Biomaterials. Light delivery in living tissue has several important applications including imaging, photodynamic therapy, and optogenetics.[55−58] For such applications, not only corrosion resistance and biocompatibility but also the dimensions, elastic modulus, and deformability of the light delivery system are important.[30,59−62] Whereas a number of nontoxic inorganic and polymeric materials can be used *in vivo*, the use of biologically derived materials tends to tick all of the boxes. Current state-of-the-art biologically derived waveguide materials include silk fibroin, gelatin, cellulose, and polylactic acid, among others.[63−68]

Hydrogels and biopolymers closely match the chemical and mechanical properties of living tissue and so are less likely to be recognized as foreign bodies to protective cell types. Their properties can be tuned by altering their composition to fit the specific application. Figure 1a shows how flexible 5 kDa polyethylene glycol (PEG) slabs may guide light over macroscopic distances (loss of 0.23 dB/cm), whereas 0.5 kDa PEG exhibits an optical loss of ∼25 dB/cm.[60] Hydrogels are particularly suitable as implant materials because they allow local cells to invade and interact directly with the optical component.[68] This reduces the likelihood of forming thick scar tissue around the waveguide if implanted, which can significantly impede the penetration depth of the optical signal. An example of such cell integration within hydrogel is shown on Figure 1b, where breast cancer cells are embedded in an agarose waveguide and detected by confocal microscopy. Many hydrogels such as agarose and gelatin can also be degraded by cells, eliminating the need for surgery to remove the implant after the therapy is completed.[69−71] However, hydrogels are difficult to fabricate in small dimensions with sufficiently low loss for high-resolution light delivery because their refractive index is close to that of living tissues.[61]

Silks are another example of low-loss, easily patterned biomaterials. Silk, which can be easily reconstituted from the cocoons of certain silkworms and spiders, has excellent optical and mechanical properties.[72−74] The refractive index of both silkworm and spider silks ($n \approx 1.55$ at 1550 nm) rivals or exceeds the index of most polymers. Whereas the native fiber form of silk naturally lends itself to guiding light,[75] silk is also amenable to waveguiding in integrated devices, as shown in Figure 1c for printed silk waveguides. Silk fibroin solution can be spun into thin films and patterned via stamping, molding, or printing.

https://dx.doi.org/10.1021/acsphotonics.0c00983
ACS Photonics XXXX, XXX, XXX−XXX

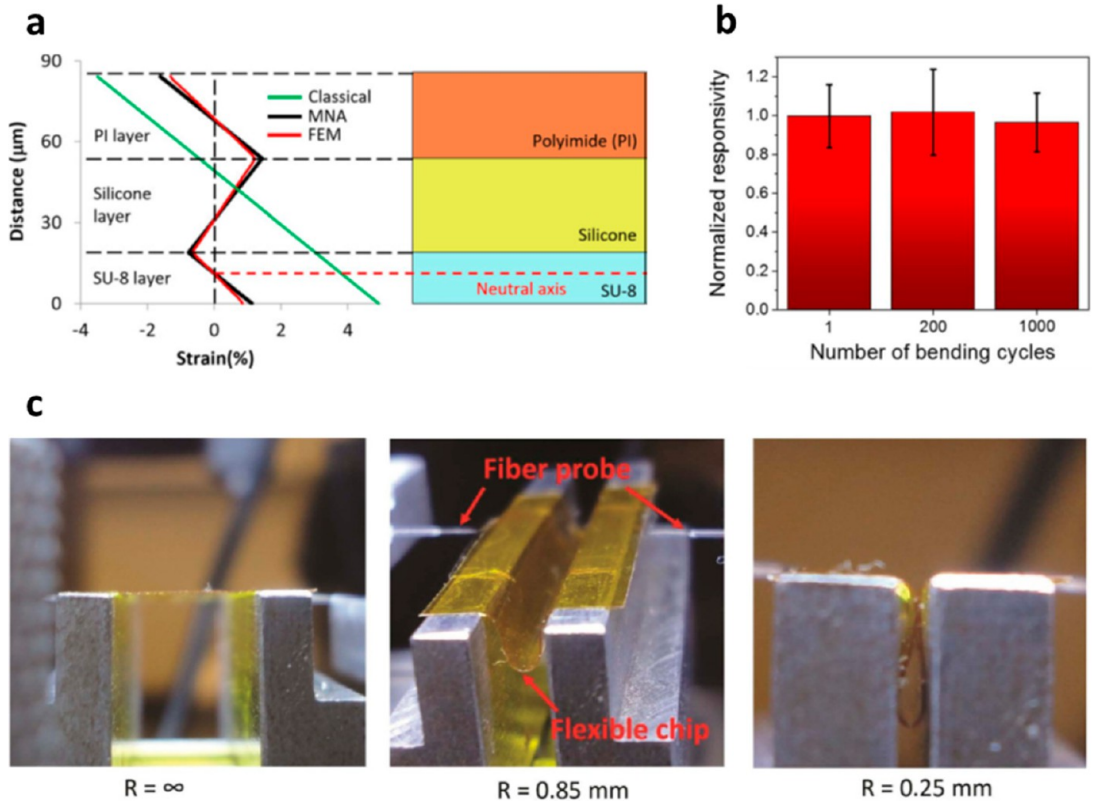

Figure 2. Multineutral axis (MNA) design enables foldable photonics. (a) MNAs emerge when a soft midlayer is sandwiched by two much stiffer layers. Adapted with permission from ref 85. Copyright 2016 The American Ceramic Society and Wiley Periodicals, Inc. (b) Normalized responsivity of a flexible photodetector after multiple bending cycles at $R = 0.8$ mm. Reprinted with permission from ref 99. Copyright 2018 Optical Society of America. (c) MNA flexible waveguide under testing at different bending radii. Reprinted under the terms of the CC-BY 4.0 Creative Commons Attribution License from ref 98. Copyright 2015 Springer Nature.

Inorganic Materials. Inorganic materials such as semiconductors,[78−80] metals,[81−84] and glasses[85−89] open up additional material design space for flexible photonics, offering properties highly complementary to those of organic materials: high refractive indices for strong optical confinement, large free electron density enabling plasmonic enhancement, electro-optic or magneto-optic activity, and superior thermal and chemical stability. These materials, however, are often rigid in their bulk form, with elastic moduli ranging from tens to hundreds of gigapascals—orders of magnitude larger than those of organic materials. Moreover, most inorganic semiconductors and glasses are intrinsically brittle and tend to fracture at tensile strains of no more than a few percent. The potential vast mechanical property mismatch mandates judicious configurational engineering when integrating inorganic materials onto flexible substrates.

Even the stiffest materials can be made highly compliant to bending when thinned down to less than a few hundred nanometers, for instance, semiconductor nanomembranes (NMs).[90−92] This can be well understood through the Euler−Bernoulli beam theory (EBT) which proves that the bending rigidity scales with beam thickness cubed and the allowable bending radius is proportional to beam thickness. An extreme example is 2D materials such as graphene: Their single-atom-layer configuration and the ensuing large mechanical flexibility facilitate integration on flexible photonic platforms.[93,94]

Flexible electronic devices are customarily created by sandwiching an NM near the neutral plane of a bending sheet where all strains vanish.[12] This strategy, however, is not always applicable to flexible photonics. For many optical applications such as evanescent sensing and coupling, it is desirable to locate the photonic devices close to the substrate surface. Moreover, the encapsulation of active photonic components in flexible polymers, which are normally poor heat conductors, can be problematic.

A multineutral axis (MNA) design has been proposed to resolve the challenge, where a soft laminate is sandwiched between two much stiffer polymer layers to form a composite substrate that no longer follows the EBT.[95−97] In this case, a neutral axis emerges in each stiff layer due to the decoupling effect (i.e., significant shear strain) in the soft midlayer. Through varying the elastic properties and thicknesses of the layers, the locations of neutral axes can be tuned to allow for flexible placement of the photonic devices in the stack. Figure 2a shows the difference between the predictions of the EBT (classical) and those of the new MNA theory, which match well with finite element modeling (FEM) results. The multiple neutral axes are also visible. Using this approach, photonic components that can sustain repeated small-radius bending have been demonstrated.[97−99] Device performances such as optical loss for waveguides, quality factor for ring resonators, and responsivity for photodetectors, were shown to be reproducible under repeated bending at submillimeter bending radii (Figure 2b,c).

Transforming inorganic materials into stretchable photonic devices involves a different design paradigm. The rigid materials must be patterned into serpentine ribbons[100,101] or

https://dx.doi.org/10.1021/acsphotonics.0c00983
ACS Photonics XXXX, XXX, XXX−XXX

discrete islands[102−104] to accommodate device elongation. The first approach relies on mechanical design and material engineering to warrant reproducible optical properties upon stretching. The strain in the waveguiding material is relieved by both Euler bends and an encapsulating epoxy (Figure 3a). The

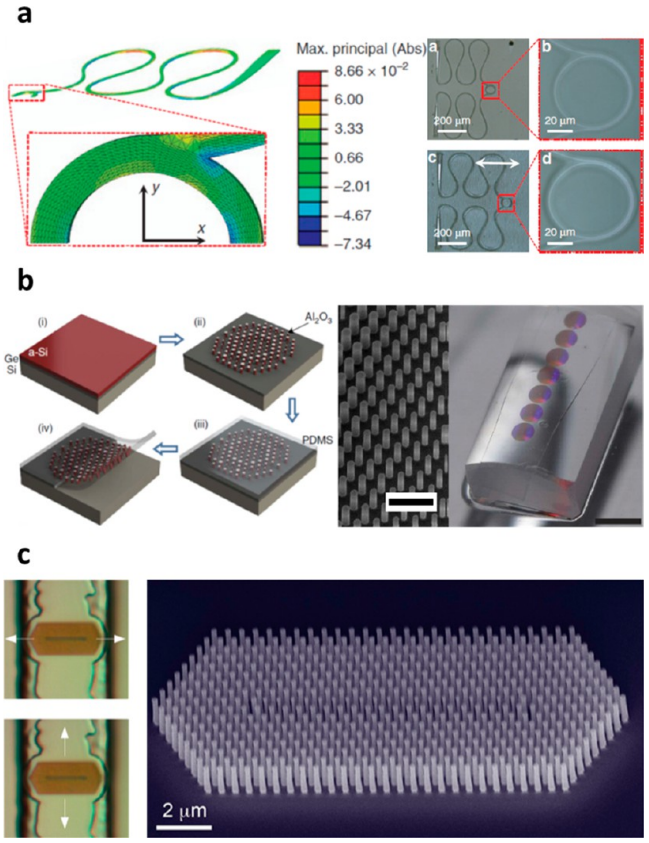

Figure 3. Designs for stretchable photonics. (a) Serpentine waveguides in Euler spiral geometry relieve strain while mitigating radiative optical loss in stretchable chalcogenide glass ring resonators encapsulated in epoxy and PDMS. Reprinted under the terms of the CC-BY 4.0 Creative Commons Attribution License from ref 101. Copyright 2017 Springer Nature. (b) Etched silicon posts are embedded in PDMS and conformed to cylindrical surfaces. Reprinted under the terms of the CC-BY 4.0 Creative Commons Attribution License from ref 102. Copyright 2016 Springer Nature. (c) Silicon nanowires embedded in PDMS demonstrate reversible frequency tuning at telecom bandwidths when stretched transversely. Reprinted with permission from ref 104. Copyright 2012 American Chemical Society.

second approach ensures minimal damage to the optical material upon stretching by concentrating the strain in the elastomer in-between islands. To achieve high-quality fabrication of the small discrete islands and encapsulation in the elastomer, a transfer technique is often adopted, as pictured in Figure 3b and discussed in more detail in the Fabrication Techniques section. Upon deformation, the large change in island spacing significantly modifies the device's properties. For the metalens shown in Figure 3b, whose final, static shape is known, this change is taken into account at the design stage such that the deformed lens yields the desired focusing. Inversely, dynamic changes are used to reversibly tune the resonance position of the photonic crystal shown on Figure 3c. The holistic mechanical and optical approach required in such cases of large stretchability is discussed in more details in the Missing Pieces: Enabling Technologies section.

Many emerging photonic designs also necessitate the combination of multiple materials to bestow unique optical properties that are otherwise hard to access. Examples include epsilon-near-zero (ENZ) and hyperbolic media, both of which entail multilayer formation on flexible substrates.[105] However, the integration of these materials with flexible substrates still remains a major challenge. One of the most commonly used fabrication approaches is layered epitaxial growth, which demands a few critical criteria for the substrate such as lattice matching, processing temperature, and precursor conditioning, which are difficult to meet with flexible substrates.[106−108] Another issue is the postdeposition processing, especially thermal annealing, which remains challenging for polymer substrates such as epoxy and PDMS, as they cannot survive high-temperature processes. For example, transparent conducting oxides (TCOs) such as indium tin oxide (ITO) and aluminum zinc oxide have been demonstrated as cost-effective and well-functional ENZ metamaterials.[109−112] Yet even though the TCO deposition process stays feasible for flexible substrate integration, the postdeposition annealing (thermal) would cause deformation, strain, and interface delamination on flexible substrates.

FABRICATION TECHNIQUES

A diverse set of processing techniques exists for the fabrication of flexible and stretchable photonic devices (Figure 4). The choice of a particular processing route results from the combination of the materials requirements, desired performance, and specifics of the intended functionality. Process flows may generally be divided between fabrication on a free-standing flexible substrate and fabrication on a rigid carrier before transferring to a soft substrate.

Perhaps the closest to traditional fabrication on planar rigid substrates, transfer printing (also called "stamp printing") involves processing the optical material of interest on a handling substrate before transferring the structure onto another soft or 3D substrate.[113−121] This process is preferred for crystalline materials, which require epitaxial growth and thus have to be heterogeneously integrated onto polymeric substrates. A representative process flow is illustrated by Figure 4a. It typically starts with a rigid wafer comprising the layer of interest on top of a sacrificial layer, for example, a buried oxide (BOX) layer. The top layer is patterned into the desired final geometry using conventional techniques. The sacrificial layer is then undercut by selective etching, thus releasing the top membrane, which remains in place if only partially undercut or thin enough to be held by van der Waals forces if fully undercut. The transfer to the flexible substrate can then happen by two methods: In a direct flip transfer, the released membrane is directly put into contact with the final substrate; in a stamp-assisted transfer, the membrane is first peeled off by a stamp, then pressed against the final substrate while the stamp is slowly released from the membrane. Limitations of this technique include its limited throughput and yield due to the restricted surface area, the use of a sacrificial layer, and the multiple steps involved in the transfer. It is also sensitive to the quality of the target surfaces.

In contrast, amorphous materials allow for monolithic integration,[38,45,97,98,122] that is, fabrication directly on the flexible substrate, as illustrated by Figure 4b. A rigid handler is used throughout the fabrication process. The target flexible

https://dx.doi.org/10.1021/acsphotonics.0c00983
ACS Photonics XXXX, XXX, XXX−XXX

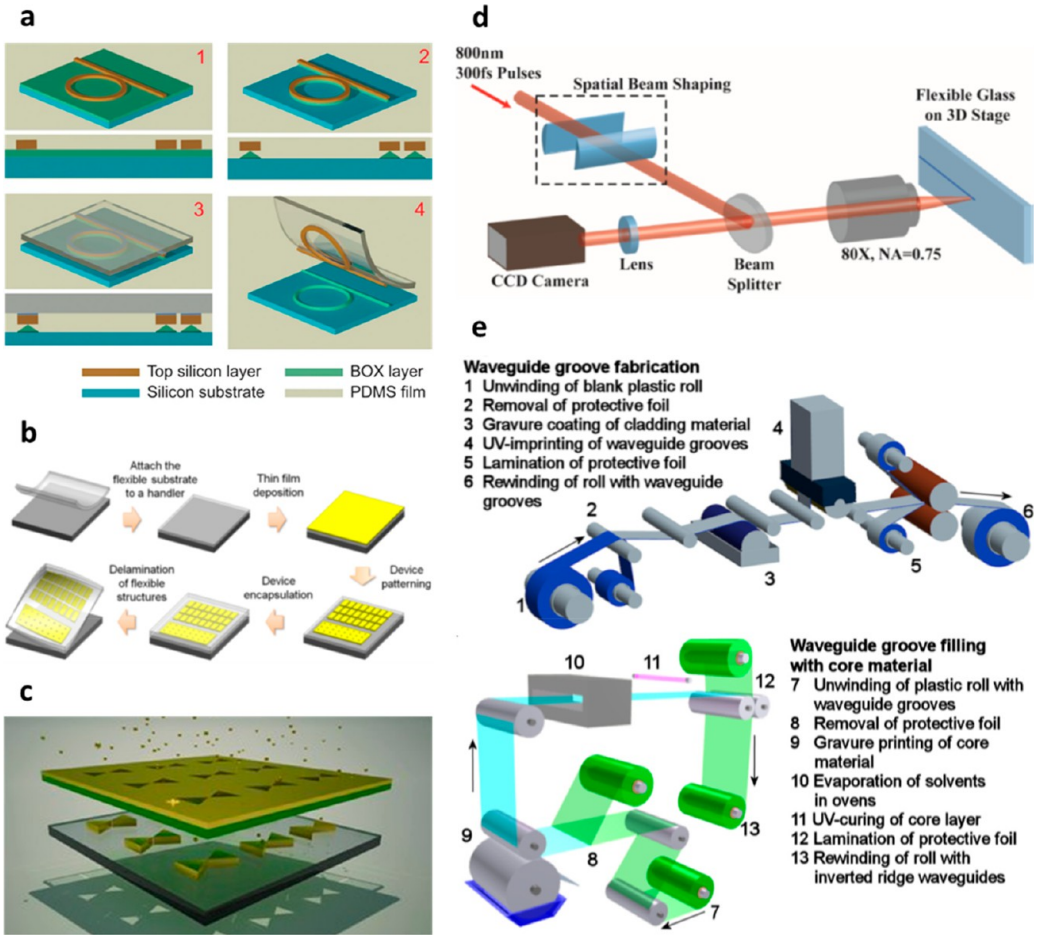

Figure 4. Fabrication techniques for flexible photonics. (a) Transfer printing process flow, with a crystalline waveguiding material. Reprinted with permission from ref 78. Copyright 2012 Springer Nature. (b) Monolithic integration process flow, with an amorphous waveguiding material. Reprinted with permission from ref 96. Copyright 2013 Optical Society of America. (c) Nanostencil lithography allows for high-throughput deposition of metals, dielectrics, and organics on polymeric substrates without thermal constraint. Reprinted with permission from ref 81. Copyright 2011 Wiley-VCH. (d) Direct writing of waveguide by laser in a flexible glass substrate. Reprinted with permission from ref 128. Copyright 2015 Optical Society of America. (e) R2R fabrication unit of epoxy waveguides in acrylate flexible cladding by stamping. Reprinted with permission from ref 135. Copyright 2016 Optical Society of America.

substrate is first deposited or attached to the handler. The optical material is then deposited and patterned using conventional techniques, as discussed later. Finally, if desired, another layer of polymer is deposited to encapsulate the device before the entire structure is peeled off from the handler.

Most, if not all, of the conventional deposition and patterning techniques may be used in the flexible photonics fabrication process, taking into account the specific requirements of the materials and the subsequent steps. For example, deposition and patterning on polymeric substrates are limited to temperatures below the polymer's glass-transition temperature, which usually ranges from 100 to 300 °C. This may result in degraded electrical and optical properties as well as mismatch-strain-induced structural damage due to large differences in the coefficient of thermal expansion.[101]

Methods that circumvent these constraints are particularly suited to flexible photonics. Nanostencil lithography (NSL) is a shadow-mask patterning technique (Figure 4c) that allows for wafer-scale, resist-free patterning of sub-100 nm structures on any substrate.[123−125] Because NSL encompasses both deposition and patterning and does not require any resist, it reduces the number and complexity of fabrication steps. Direct-write techniques such as laser writing (Figure 4d) or printing present the same advantage of being resist-free and can be adapted to a wide range of substrates. However, they are somewhat limited to larger pattern dimensions and specific materials, especially in the structuring of biological materials.[117,126−130] Stamping and molding are high-throughput methods adaptable to R2R manufacturing, allowing device production to be scaled up to industrial levels.[131−134] Figure 4e shows a unit used to fabricate over 200 m of a 15 cm wide roll of single-mode chemical sensors with a nickel stamp. The stamp is used to create a groove in the flexible substrate, which is then filled with the higher index waveguiding polymer to create an inverted ridge waveguide.

APPLICATIONS

Conformal Integration onto Curvilinear Surfaces. The integration of flexible and stretchable optical elements on a 3D curvilinear platform can transform conventional optical and photonic systems into advanced 3D architectures with new functionalities. The applications of optical devices conformally integrated on substrates with unconventional geometries include imaging (Figure 5a),[29,136] optical cloaking (Figure 5b),[137−141] optical illusions,[136] as well as biomedical and chemical sensing (Figure 5c).[142−145] Conformal metasurfaces

https://dx.doi.org/10.1021/acsphotonics.0c00983
ACS Photonics XXXX, XXX, XXX−XXX

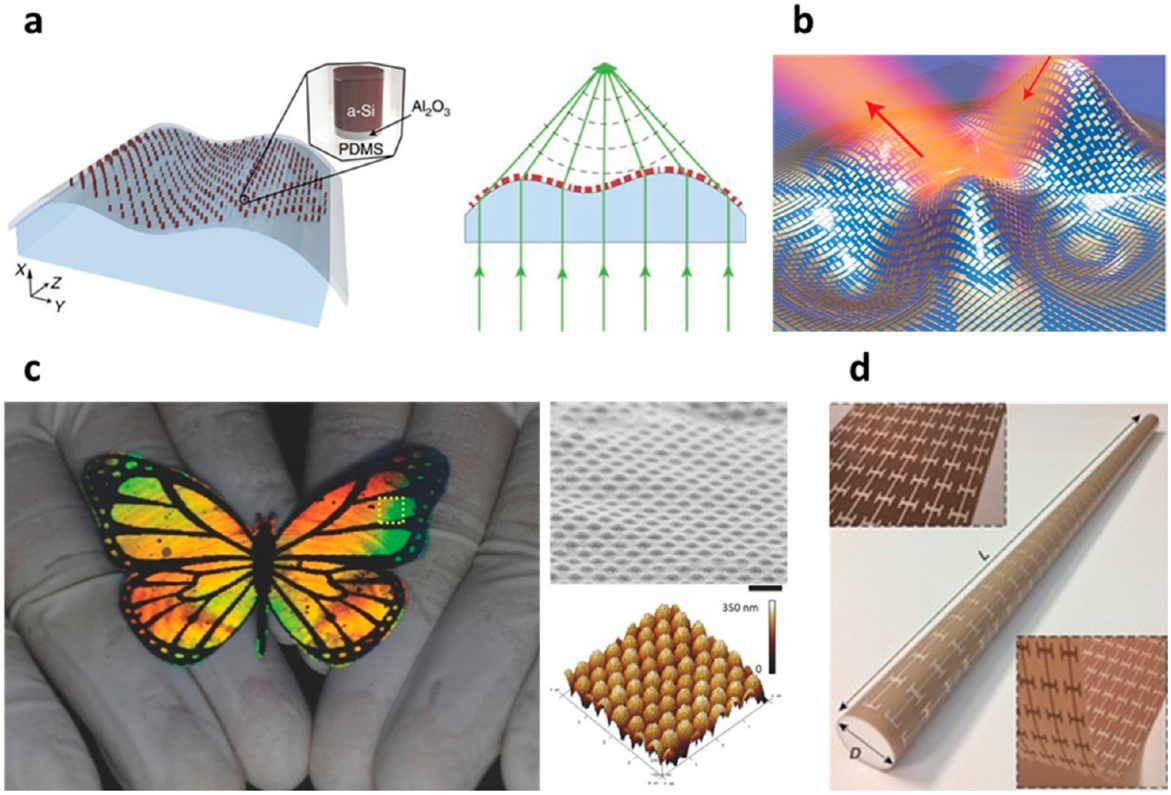

Figure 5. Conformally integrated optical devices. (a) Conformal metasurface for imaging. Reprinted under the terms of the CC-BY 4.0 Creative Commons Attribution License from ref 102. Copyright 2016 Springer Nature. (b) Optical cloaking. Reprinted with permission from ref 137. Copyright 2015 AAAS. (c) Flexible plasmonic metasurface for molecular sensing. Reprinted with permission from ref 83. Copyright 2016 Wiley-VCH. (d) Waveguide made of a Teflon rod coated by a metasurface layer. Reprinted under the terms of the CC-BY 4.0 Creative Commons Attribution License from ref 146. Copyright 2017 Springer Nature.

are also used as coating layers on dielectric waveguides to provide enhanced control of various properties of electromagnetic waves (Figure 5d).[146]

The challenge of integrating flexible photonic devices with curvilinear surfaces can be overcome by borrowing ideas from stretchable electronics. For example, large-area stretchable devices can be transferred to complex 3D surfaces by transfer printing techniques such as water- or balloon-assisted transfer.[147−149] Kirigami-inspired device design enables nonstretchable but flexible devices to conform to curvilinear surfaces with minor stretching (e.g., <0.5%) and minimal loading to the biotissues.[150−152] Theoretical results for conformability criterion or prediction on rigid or soft corrugated substrates are also available.[15,153,154]

Flexible metasurfaces present an excellent case to demonstrate the benefits of conformal integration. Traditional conformal free-space optical systems, such as those designed for medical devices and aerodynamic objects,[155] face the challenge of simultaneously meeting the requirements for optical performance and packaging on curved surfaces in a compact manner. Usually additional optical elements and system complexity are needed to compensate for the geometry compliance. Metasurfaces, which consist of optically thin, subwavelength arrays of nanoantennas, can provide on-demand control of the phase, amplitude, and polarization of an incident beam (Figure 5a).[156,157] When conformally integrated onto a nonplanar substrate, their capability to arbitrarily manipulate wavefronts allows for the compensation of any local phase deviation induced by the substrate, therefore effectively decoupling their optical functionality and substrate geometry. For example, a dielectric metasurface consisting of a-Si nanoposts embedded in a PDMS substrate is designed and conformally integrated on cylindrical substrates to demonstrate a lensing functionality regardless of the substrate shape.[102] The conformal integration of metasurfaces or metamaterials further enables the modification of the optical responses of an object. For instance, an ultrathin optical skin cloak is demonstrated, which can be wrapped over an arbitrarily shaped object to achieve invisibility. This metasurface-based cloak is designed to provide phase compensation to restore the reflected light from a 3D object (Figure 5b).[137]

The capability to design, fabricate, and integrate conformal optics onto substrates with arbitrary geometries is essential to decoupling optical functionality from the features of the substrate as well as enhancing light−matter interactions. An analytical method for designing conformal metasurface optics has been introduced,[136] which provides a versatile framework for wavefront manipulation on arbitrary substrate geometries. However, it should be noted that most of the existing design approaches for stretchable and flexible conformal metasurfaces and metamaterials do not fully account for stress-induced strain−optical coupling during the fabrication and integration processes of nonplanar metasurface devices. As discussed in the Missing Pieces: Enabling Technologies section, a holistic design approach that properly accounts for such an optical property change due to deformation is necessary for optimal device design.

https://dx.doi.org/10.1021/acsphotonics.0c00983
ACS Photonics XXXX, XXX, XXX−XXX

Optical Interconnects and Photonic Packaging. Large-scale data centers and high-performance computers (HPCs) are becoming increasingly limited by the capacity of interconnects due to the rapidly increasing power consumption and bandwidth demands driven by the rigorous down-scaling of complementary metal−oxide−semiconductor (CMOS) critical dimensions in accordance with the Moore's law. As a result of the continuing bandwidth scaling, optical interconnects (OIs) have been implemented at ever decreasing communication distances.[158,159] Despite the widespread recognition of fiber-based OIs as the interconnect solution at the rack and board levels, no mature technical pathways are currently available to meet the key performance metrics for interchip OIs.[160−162]

Optical links based on flexible waveguides offer several unique advantages: (1) Flexible waveguides can provide scalable, high bandwidth density sufficient for chip-level OIs in future technology nodes,[160] (2) multiple thin sheets of waveguides can be stacked together to further improve the link density,[163,164] (3) mechanical flexibility accommodates misalignment between chips surface mounted with moderate positioning accuracy (e.g., 5 μm) on carriers or printed circuit boards,[161,162] and (4) low-profile flexible links are compatible with flip-chip assembly and ease subassembly designs with more degrees of freedoms than rigid links (Figure 6b).[162] Whereas no standard testing methods have been formulated for flexible optical components yet, the IPC (Association Connecting Electronics Industries) standard IPC-TM-650 (Flexural Fatigue, Flexible Printed Wirings) can be referenced as a guideline.[165] The standard recommends that flexible ribbon cables should sustain bending deformation at 6 mm radius for 1000 cycles or more without fracturing. The waveguides must also withstand temperature fluctuations from 15 to 85 °C given their proximity to CMOS chips.

There has been significant development in flexible OIs in recent years. Polymer waveguides were initially developed for multimode operation coupled to 850 nm vertical-cavity surface-emitting lasers (VCSELs) and have demonstrated efficient out-of-plane coupling capabilities essential for compact optical interfacing.[37,163,166,167] Stretchable PDMS waveguides fabricated by replication have also been demonstrated.[100] The need for higher bandwidth density and integration has led to the development of flexible single-mode waveguides with operation wavelengths extended to 1310 and 1550 nm (Figure 6a).[33,163,168] For example, IBM Research has developed low-loss single-mode polymer waveguides and adiabatic optical couplers for integration with Si photonics devices.[163] Large-scale manufacture has also been demonstrated by depositing polymer layers using doctor-blading followed by a UV laser direct-writing or proximity-mask-lithography process to define waveguides. Panel-sized flexible single-mode waveguide arrays are realized with dimensions up to 450 mm × 300 mm.[33] As discussed in the Inorganic Materials section, high-index-contrast glass waveguides fabricated on a flexible platform have also been demonstrated. Such a flexible waveguide fabric is further integrated with III−V active photonic devices via hybrid integration, thus paving the path toward a fully integrated flexible OI platform.[96,99,162]

Photonic packaging faces the same coupling challenges as OIs and can thus benefit from flexible links in the same ways enumerated above. The three main solutions for optical coupling are diffractive, adiabatic, and butt coupling.

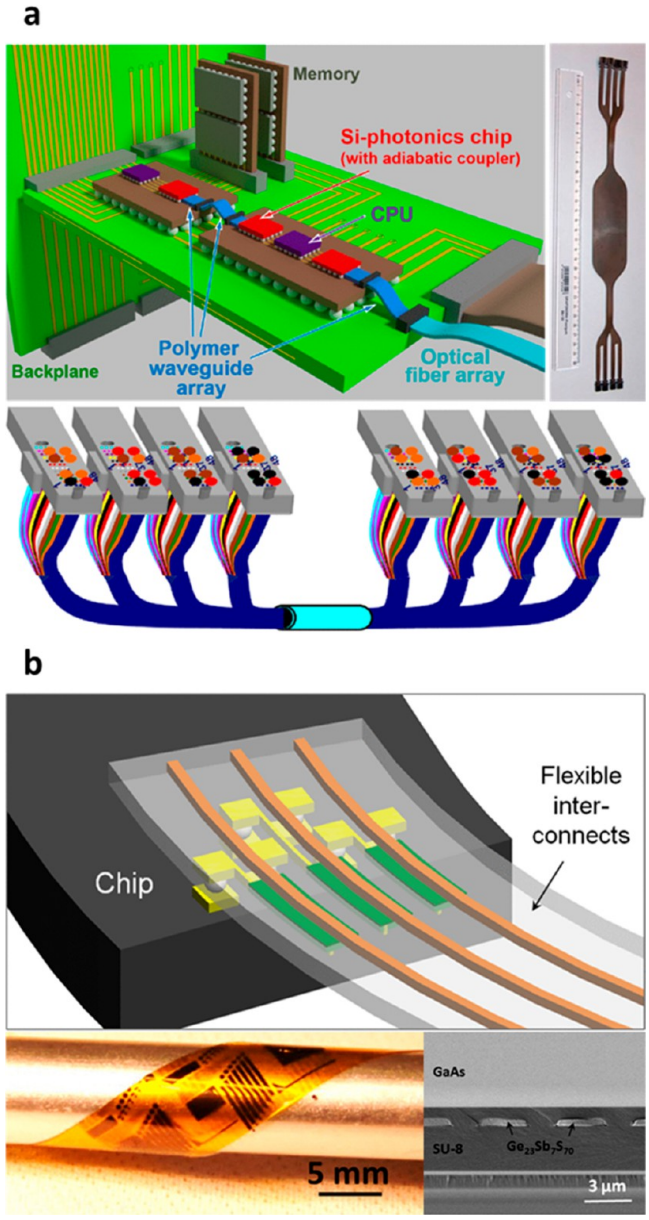

Figure 6. Flexible optical interconnect technologies. (a) IBM/Corning siloxane-based flexible waveguides. Single-mode waveguides adiabatically couple to a silicon photonics chip (top left). Image (right) and schematic (bottom) of eight-layer interconnected siloxane waveguides fabricated with the latest siloxane waveguide technology. Reprinted with permission from refs 33 and 163. Copyright 2018 and 2013, respectively, IEEE. (b) Glass embedded in polyimide/silicone/polyimide trilayers forming flexible interconnects. The flexible interconnects bonded to a semiconductor die (top). Flexible waveguide devices wrapped around a mandrel (bottom left). Cross-section of the bondable die (bottom right). Reprinted with permission from ref 162. Copyright 2013 IEEE.

Diffractive and adiabatic coupling benefit from larger alignment tolerances but require high index contrast and effective index crossing,[169,170] leaving butt coupling as the only method able to combine different materials in a single system. A major hurdle is, however, the additional requirement of tight alignment tolerances to ensure low-loss transmission from one optical device to the next. Because the accuracy of standard pick-and-place tools, ∼10 μm, is much larger than the 1 to 2 μm (or below) precision needed to efficiently align to

https://dx.doi.org/10.1021/acsphotonics.0c00983
ACS Photonics XXXX, XXX, XXX−XXX

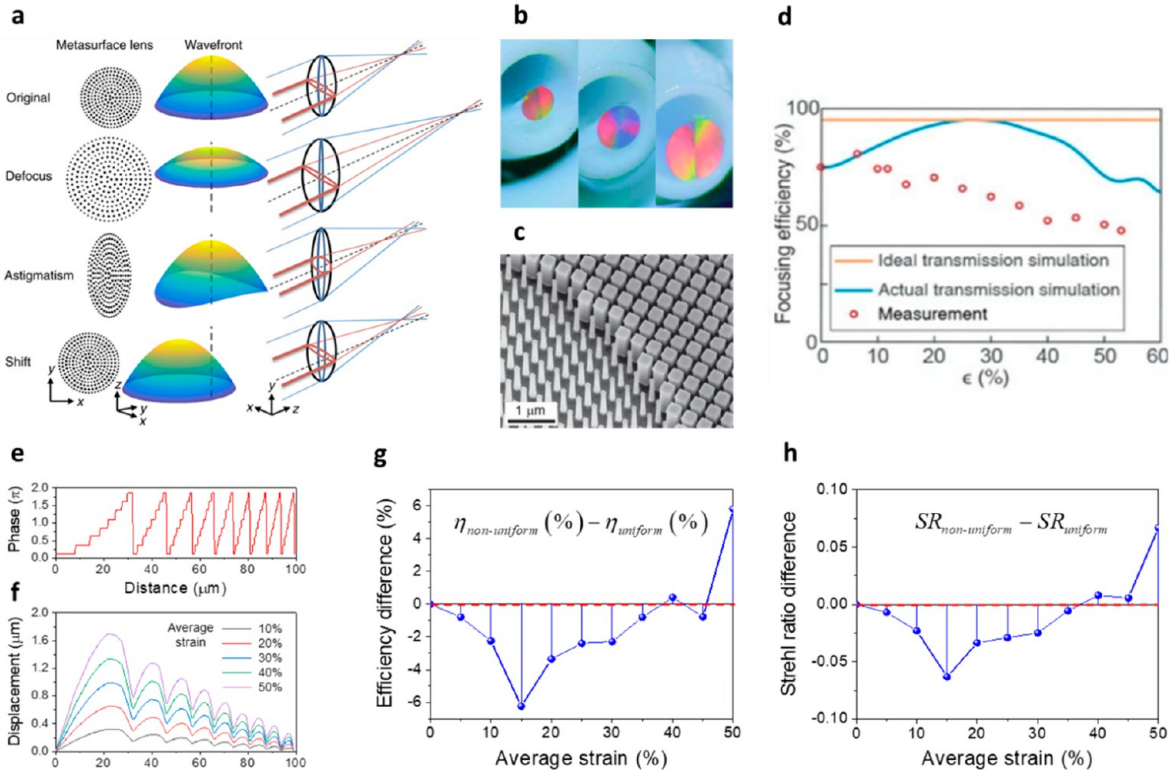

Figure 7. (a) Design principles of stretchable metasurface for active function tuning. Reprinted from ref 179. Copyright 2018 The Authors, some rights reserved; exclusive licensee AAAS. Distributed under a CC-BY-NC 4.0 Creative Commons Attribution License. (b) Optical and (c) SEM images of a stretchable metalens comprising a-Si nanoposts embedded in PDMS. Reprinted with permission from ref 103. Copyright 2016 Wiley-VCH. (d) Focusing efficiency of a metalens under various strain values. A numerical model examining both the mechanical and optical impacts on a stretchable metasurface due to strains: (e) phase distribution under 0% strain, (f) difference between simulated meta-atom positions and those of ideal uniform distribution under different strains (*x*-axis indicates the position of meta-atoms under 0% strain), (g) simulated focusing efficiency, and (h) Strehl ratio under the nonuniform distribution of meta-atoms.

single-mode waveguides, specific strategies are needed to avoid using higher precision tools that would significantly increase the packaging cost. Mechanical flexibility allows flexible links to move and change shape to maximize the coupling efficiency, thereby relaxing the alignment tolerances. An example of a low-cost, high-volume approach based on flexible links consists of using lithographically defined alignment features that guide flexible waveguide ribbons into place.[171]

Photonic Tuning and Strain Sensing. Controlled mechanical deformation furnishes a uniquely advantageous approach for tuning photonic structures, as the large strain attainable in flexible photonic structures (in some cases exceeding 100%) enables extreme broadband tuning or reconfiguration between two drastically different optical states. Optical metasurfaces formed on flexible or stretchable platforms may notably leverage their pixelated planar device architecture to realize reconfigurable flat optics.[172] Distinct from waveguide structures, the discrete meta-atom distribution presents additional variables. Some notable examples include wavelength tuning of resonant optical structures,[78,104,173−177] strain-switchable metasurface holograms,[178] adjustable metalenses,[82,103,179] and tunable coloration.[180−182]

The strain−optical coupling effect can also be leveraged in the other direction for strain or deformation sensing.[183−185] Compared with electrical strain gauges and fiber Bragg grating (FBG) sensors, flexible photonic sensors claim unique advantages such as high sensitivity,[97] a fast and highly reversible response, immunity to electromagnetic interference, minimal temperature sensitivity with proper thermal compensation,[186] multidirectional strain sensing capability,[187] and a large capacity for multiplexing.

Chemical and Biological Sensing. The interaction of the evanescent tail of a confined waveguide mode or the electric or magnetic field of a metasurface with its environment is useful in chemical detection applications. The analyte may be flowed over the optical device and detected as is,[188,189] or binding sites may be used to trap the analyte on the sensor surface.[135,190] Chemical sensor flexibility is key not only for wearable or implantable sensors but also to reduce the cost of photonic sensors by fabricating them with traditional R2R processing. Several sensor types have shown good sensitivity in chemical detection on flexible platforms, most notably interferometers and resonators for refractometry sensing and metamaterial surfaces for electromagnetic resonance-based chemical sensing.

The most common interferometers used in chemical sensing are Mach−Zender and Young's interferometers (MZI and YI, respectively). In a YI, separate output signals from the reference and detection waveguides interact with each other to produce fringes that vary with the change in the refractive index of the detection waveguide. Flexible YIs have been used in the detection of glucose with sensitivity on the order of 10^{-6} RIU.[135] In an MZI, the reference and detection signals are coupled back into the same waveguide, and the degree of constructive or destructive interference between the two signals is analyzed. Silicon-on-plastic and all-polymer flexible

https://dx.doi.org/10.1021/acsphotonics.0c00983
ACS Photonics XXXX, XXX, XXX−XXX

MZI sensors have been fabricated with excellent sensitivity to changes in their mechanical and chemical environments.[78,188]

Ring resonators and photonic crystal cavities rely on shifts in their resonant wavelength for chemical detection. Several resonators patterned via R2R or R2R-compatible methods have been produced with high sensitivity, as indicated by quality factors on the order of 10^4 to 10^5.[3,64,126,133] It should be noted, however, that for refractometry-based flexible sensors, it is important to decouple index changes resulting from analyte binding and mechanical deformation. Understanding and suppressing the strain−optical coupling of the sensor device (e.g., via local substrate stiffening) is therefore critical, as will be discussed in more detail in the Missing Pieces: Enabling Technologies section.

Similarly, resonance shifts of metasurfaces can also be used for sensing. Two chief mechanisms in flexible metasurfaces lead to resonance peaks in their transmission spectra: Mie resonance and plasmon resonance.[143−145] The geometry of such metasurfaces can be tuned to achieve both magnetic and electronic resonances and to control their position. Gold, titanium/gold, and silver split-ring resonators have been fabricated on flexible platforms of PDMS, paralyne-C, and poly(ethylene napthalate) with operation from visible to IR wavelengths.[142−145] The magnetic resonance of such metamaterials shows a highly sensitive response to surrounding chemical and strain variations, offering a promising approach for chemical and biological sensing.

MISSING PIECES: ENABLING TECHNOLOGIES

Holistic Mechanical and Optical Design. In flexible and stretchable integrated photonic devices, the strain/stress field variation induced by physical deformation usually leads to changes in the optical property of the device, often via three effects:[79,191] the waveguide effective index change, the waveguide length change, and the refractive index change of the waveguide core and cladding materials. The first two are due to dimensional variations caused by strain, whereas the refractive index change is due to the photoelastic effect. The strain−optical coupling of waveguide devices has been analyzed by several groups.[38,79,191,192] Recently, a more generalized, rigorous analytical model was established and experimentally verified, enabling the quantitative prediction of stress−optical coupling behavior in waveguide devices without using a single fitting parameter.[101] The approach is generically applicable to arbitrary spatially varying stress profiles and waveguide geometries and enables advanced micromechanical/optical codesign strategies that further improve the robustness of the flexible/stretchable device under extreme deformation.

Mechano−photonic coupling can also be employed for deterministic photonic tuning through mechanical strain, as previously discussed. For active tuning, meta-atoms are usually embedded inside a soft matrix, and the output wavefront is reconstructed via lattice deformation. The stretchable metasurfaces are further integrated on curvilinear surfaces of traditional refractive or reflective optics[193] or coupled to other flexible photonic components to achieve additional functionalities.

In these approaches, soft substrates are typically employed to allow continuous variation of the meta-atom spacing, whereas rigid meta-atoms made from semiconductors or dielectric materials possessing much larger elastic moduli are used to minimize the geometric deformation of the unit cells. The tunable optical functionalities are subsequently predicted based on the designed lattice deformation pattern across the entire metasurface, as shown in Figure 7. While being an elegant method to realize tunable functionalities, completely decoupling the mechanical and optical effects sometimes leads to nonoptimal optical performance during the deformation process. For example, the stretchable lens in ref 103 shows strain-dependent optical efficiencies, which deviate from numerical models (Figure 7d). Here we note that in addition to potential fabrication imperfections, two primary factors could contribute to the optical performance degradation: (1) the nonuniformity of the strain distribution across a stretchable metasurface, which results in lattice deformation and phase errors, and (2) the change in inter-meta-atom coupling condition that affects the unit-cell transmission and the phase shift. Here, as shown in Figure 7e−h, we utilize mechanical and optical simulations to illustrate such impacts and compare them with the case based on the conventional assumption of a uniform strain distribution.

In this model, Si nanopost structures are embedded in a PDMS layer, similar to the configuration used in ref 102. Designed for 915 nm wavelength, eight nanoposts are chosen with a height of ∼700 nm and widths ranging from 100 to 250 nm, covering a 0 to 2π phase shift. The lattice constant at 0% strain is 380 nm. An aberration-free metalens with a diameter of 200 μm is designed assuming a hyperbolic phase profile and a focal length of 610 μm at 0% strain (Figure 7e). The metalens is then stretched up to 50% strain, while the local strain field and resultant displacement of individual meta-atoms are simulated via FEM using the commercial software ABAQUS v6.14. The optical performance of the metalens is evaluated using a hierarchical combination of FEM (COMSOL Multiphysics) and the Kirchhoff diffraction integral. On the subwavelength scale, full-wave FEM simulations are implemented to model the unit cell responses at different lattice distances under strain. At the macroscopic system level, the diffraction integral method incorporates the simulated unit-cell optical responses and lattice distance distribution, which enables the computationally efficient validation of the focusing characteristics of the entire metalens. For simplicity, both optical and mechanical simulations are performed in 1D.

Figure 7f shows the difference between the simulated individual meta-atom positions and those assuming a uniform strain distribution under different strain values. The simulation results clearly indicate a nonuniform distribution of the meta-atoms, in particular at larger strain values. This effect is primarily due to the periodic distribution of meta-atoms with different sizes that results in a large effective modulus contrast at local sites. It can be observed that in some circumstances, the deviation is comparable to or larger than the lattice constant in that strained state, introducing phase errors and effectively deforming the entire phase profile. As a result, when compared with the uniform distribution cases, optical simulations of the entire metalens incorporating the displacement effect reveal optical efficiency variations due to the strain (over ±6% efficiency change), as shown in Figure 7g. We further analyze the focal spot profiles and quantify their focusing performance via Strehl ratios. As shown in Figure 7h, as the strain increases, the Strehl ratios reduce due to deformed phase profiles, leading to increased aberrations and thus degraded imaging performance.

Consequently, our analyses indicate that both optical and mechanical property changes due to strains contribute to the optical performance deterioration of a stretchable or flexible

https://dx.doi.org/10.1021/acsphotonics.0c00983
ACS Photonics XXXX, XXX, XXX−XXX

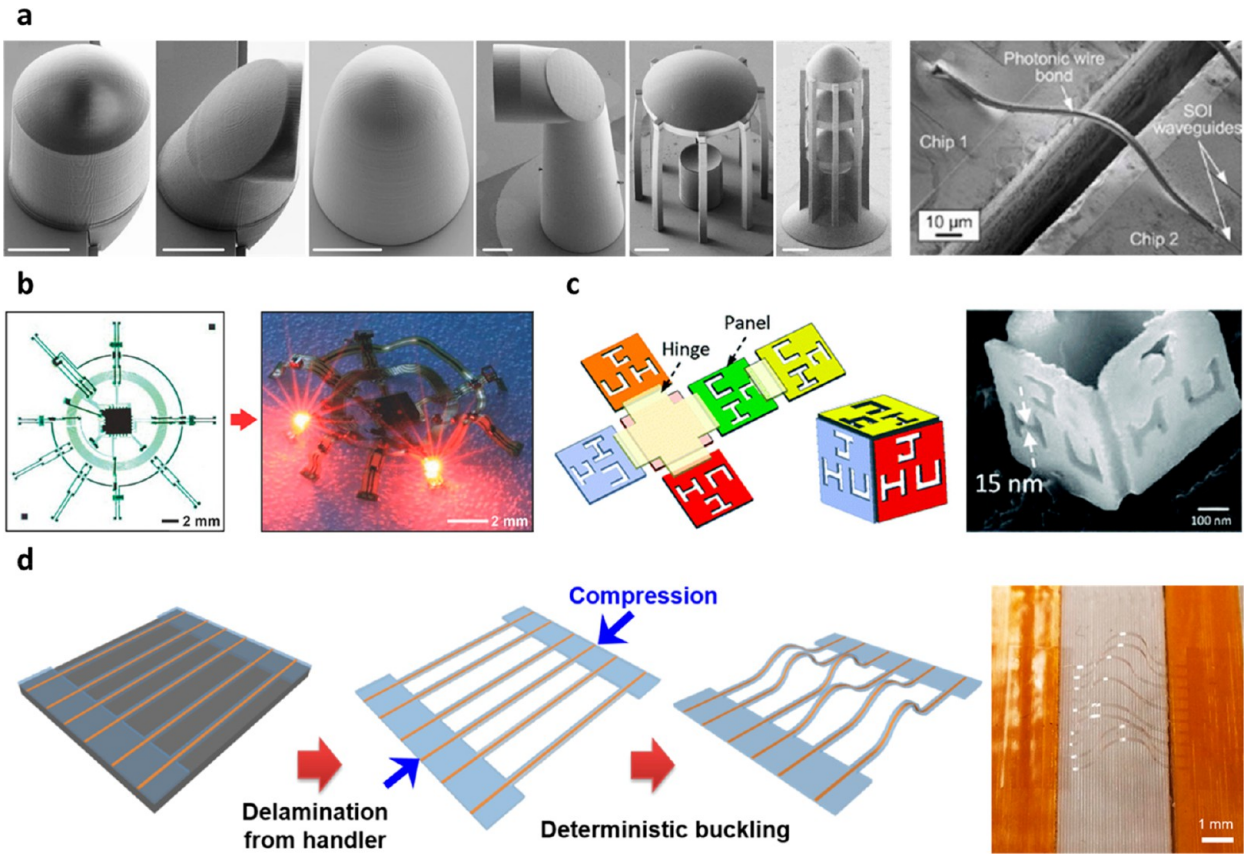

Figure 8. Fabrication techniques of 3D structures. (a) Free-form structures for free-space coupling (left) and chip-to-chip coupling (right) made by two-photon polymerization. Reprinted with permission from refs 195 and 214. Copyright 2018 Nature Springer and Copyright 2012 Optical Society of America, respectively. (b) 3D electronic platform (right) made from a 2D precursor (left). Reprinted with permission from ref 215. Copyright 2018 Wiley-VCH. (c) Cube assembled by self-folding of planar thin films. Reprinted with permission from ref 216. Copyright 2009 American Chemical Society. (d) 3D photonic sensor array fabrication process (left) and device demonstrating geometry control (right). Reprinted with permission from ref 185. Copyright 2020 Chinese Laser Press.

metasurface and thus must be accounted for during the design phase. In addition, the size difference across all meta-atoms should be minimized to reduce the contrast of effective moduli and thus improve the uniformity of strain distribution. This issue could be potentially mitigated using non-effective-medium-based meta-atoms, which assume relatively constant empty spaces between unit cells,[194] as well as a minimized inter-meta-atom coupling effect under strain.

Low-Loss, Large-Scale Flexible Waveguide Arrays. The large-scale integration of low-loss flexible waveguides is important for OIs as well as optogenetic and photodynamic therapy applications, which, respectively, require a large bandwidth density and high-resolution light delivery. Whereas single-mode flexible waveguides are essential for short-reach OIs and photonic sensing,[54] there are still a few issues waiting to be addressed to realize their full potential. In particular, the existing single-mode solutions lack compact, out-of-plane coupling capabilities that would otherwise allow dense optical interconnection and probing in the 3D space. In addition, the shrunken waveguide geometry and thus the reduced optical mode size require higher packaging precision as compared with their multimode counterparts.[168] Such functionality gaps, however, could potentially be filled by emerging additive nanofabrication techniques. For instance, two-photon polymerization (TPP) with deep subwavelength resolution could be utilized for free-form, fine-line 3D sculpting of out-of-plane waveguide coupling structures.[195−197] Such couplers could be employed to freely manipulate the optical beam in 3D space, for example, for interlayer photonic links, beam expansion for enhanced misalignment tolerance, or areal optical probing. The TPP process could be further used for nanoimprint stamp fabrication to facilitate high-volume manufacturing.[198]

The demand for mechanically flexible, low-loss, and high-resolution light delivery in biological tissues can also be addressed by developing high-density, low-loss flexible waveguide arrays. For best practice *in vivo* applications, the waveguides should be flexible enough to prevent undesired tissue damage and reactions.[199,200] Along this direction, optical waveguide materials approved by the U.S. Food and Drug Administration (FDA) include silicon, PDMS, paralyne C, SU-8, SiN, PEG hydrogels, and sapphire, all of which have already been packaged into flexible forms and successfully applied in rat models *in vivo* for proof-of-concept optoprobe applications.[46,60,200−203]

Low optical loss is another critical requirement for these light delivery solutions. In traditional photodynamic therapy, light delivery to tumors that are not near the skin is made difficult by the absorbance of visible wavelengths in tissue. Long (millimeters or more) implantable light delivery systems constructed from flexible waveguides provide a solution to this difficulty. In optogenetics, the large volume (compared with rat models) and enormous complexity of human brains mandate light delivery solutions with low propagation losses to access different parts of brain and large optical channel counts to

https://dx.doi.org/10.1021/acsphotonics.0c00983
ACS Photonics XXXX, XXX, XXX−XXX

interface with a large number of neurons. Flexible integrated photonics thus has the potential to fulfill these needs.[185]

Integration of Emerging Functional Materials onto Flexible Platforms. Functional photonic materials such as hyperbolic metamaterials (HMMs)[204−206] and epsilon near-zero (ENZ) materials[207−209] have enabled the exploration of manipulating light in localized fields as well as qualitatively different wave dynamics. Since the realization of nanoscale engineered metamaterial structures, the precision control of light has been rapidly developing for various optical applications. In recent years, with the successful demonstration of flexible electronics, research efforts have been further expanding toward developing and transferring functional photonic structures/materials onto flexible substrates.

Several successful demonstrations of this have involved HMMs. Riley et al. have solved the problem of film cracking and delamination during flexing or heating, which is typically induced when bulky and planar HMM films are transferred to flexible substrate.[210] Another application of flexible HMMs is their integration with transient technology, that is, transient HMMs composed of multilayers of water-soluble and biocompatible polymer and metal.[105] Lin et al. have fabricated transient HMMs with high-k modes and large photonic density of states (DOS) by stacking pairing layers of Au/PVA. Upon integration on a flexible substrate, the transient HMMs exhibit mechanical stability for over 3000 bending cycles.

There are several realizations of structures with near-zero parameters. However, there are two most realistic ways of obtaining a near-zero feature on a flexible substrate: doped semiconductors such as TCOs[211,212] and alternating (pairing) layered structures of metal/dielectric and all-dielectric metamaterials. For example, aluminum-doped zinc oxide and ITO exhibit a near-zero permittivity at near-infrared frequencies around the telecom wavelengths (λ = 1550 nm) and have the advantage of being CMOS-compatible and tunable platforms whose ENZ frequency can be controlled. Many demonstrations of ENZ based on TCO and layered structures in both the visible and near-IR regions have been reported in recent years. Yet a first attempt to explore ENZ material integration with flexible substrates is lacking, even though the ENZ material is designed to decouple temporal and spatial field variations in structure under geometry invariance. Both 2D ENZ cavities and 3D ENZ cavities for surface-avoiding modes have been investigated theoretically.[213] It has been demonstrated that ENZ metamaterials bear multiple solutions to wave equations, enabling the design of resonant cavities whose eigenfrequencies are invariant with respect to geometrical transformations of their external boundary. Hence they inspire new design philosophies in which the geometry of a device is not determined by, and locked to, its frequency of operation.[213] We expect the upcoming development of ENZ material for applications in flexible photonic systems, especially the CMOS-compatible ENZ platform.

3D Sensing and Light Manipulation/Delivery. Conformal 3D devices such as described in the Conformal Integration section remain limited to curvilinear geometries that are inherently 2D in topology. Nonconformal 3D photonics promises to expand the reach of photonics by enabling both the extension of traditional applications to noncurvilinear geometries and the addition of novel functionalities that cannot be attained with curvilinear surface devices.[217] However, existing fabrication methods for such 3D devices impose limitations on the achievable geometries with the currently available materials. Stacking 2D layers of optical components yields so-called 3D multilayer devices that remain inherently planar and can only interact with their environment at the surface of the device stack.[218,219] 3D direct-write techniques allow for an almost arbitrary 3D shape definition, as seen on Figure 8a, but are limited by their resolution and the lack of printable high-optical index materials required for small-footprint, high-quality waveguide devices.[117,195,214] Versatile and scalable manufacturing routes for truly 3D photonics thus remain an unmet need.

The 3D assembly of flexible, deformable structures offers a promising route to fabricate 3D integrated photonic devices. Such a concept has already been widely demonstrated in 3D electronics using rolling, folding, curving, and buckling as mechanisms[220−223] and is emerging for photonics, as shown on Figure 8. Figure 8b displays the mechanically guided formation of a 3D structure by buckling using a 2D precursor bonded at designated locations on a prestretched substrate. After releasing the prestretching of the substrate, the unbonded region pops up and forms a deterministic 3D topography due to the constrained buckling of the 2D precursor. These 3D architectures, which can be predicted by mechanical analysis, are precisely controlled by the geometries of 2D precursor and bonded sites.[13,215,224] Further improvements of this method include the inverse design of the precursor[225,226] and the reconfiguration of the 3D structure through the incorporation of shape-memory or transient materials.[227−229] To generate the stress needed for the assembly without transferring the device onto another substrate, it is possible to resort to differential stresses caused, for example, by heating, as illustrated by the folding process of Figure 8c. The Sn hinges reflow during etching, creating the torque that orients the Al_2O_3 panels.[216,230−232] The versatility and tunability of these 3D fabrication methods highlight the potential of their application to 3D integrated photonics.

Similar principles were recently applied to fabricate the first 3D integrated photonic device.[185] The fabrication process, illustrated in Figure 8d, also involves a 2D structure deformed into the desired 3D geometry. This fabrication approach for 3D integrated photonics offers a number of key advantages. First, it leverages standard planar processing technologies used in the fabrication of traditional integrated photonics, thus allowing for high-quality optical components. Second, it is readily scalable to a large number of sensing channels. Additional probing points can be created simply by increasing the number of lithographically defined strips and by multiplexing several optical sensors along each waveguide. Finally, because this platform is based on standard optical components, it allows for compatibility with common optical coupling and packaging schemes, such that devices can be readily used outside of optical laboratories.

An interesting prospect is the ability to perform material-agnostic 3D optical strain sensing. Current 3D microscale optical sensing methods such as digital image correlation, digital volume correlation, or 3D scanning confocal microscopy, as applied in traction force microscopy, rely on discerning features within a matrix to resolve spatial displacement and deduce mechanical strain.[233−237] They are therefore limited to transparent and optically homogeneous materials because optical scattering inevitably leads to image quality degradation and cross-talk with out-of-focus light. Flexible integrated photonics avoids this issue by waveguiding the light to the points of interest. This is of particular interest for thick,

https://dx.doi.org/10.1021/acsphotonics.0c00983
ACS Photonics XXXX, XXX, XXX−XXX

opaque, and heterogeneous 3D *in vitro* cell culture environments.[238−240] Flexible devices are particularly suited to detecting strain in such systems as the reduced elastic stiffness mismatch between the flexible polymer platform and these soft hydrogels (elastic moduli in the range of kilopascals to megapascals) allows for efficient strain transfer and seamless integration of the flexible device with the medium. In addition, given the wide range of physical and chemical sensing applications of optical resonators as well as the possibility of multiplexing resonators spectrally and spatially, flexible photonic devices are also amenable to monitoring a variety of parameters in a large number of locations in a distributed sensor array. A platform similar to this shown in Figure 8d thus potentially enables 3D multifunctional sensing, mapping, and light delivery, opening the door to further research in this space.

CONCLUSIONS

The examples outlined in this Perspective show the progress in flexible and stretchable integrated photonics. A wide and growing range of available materials and fabrication techniques enables geometric degrees of freedom in photonic devices, relying on both traditional and novel approaches, from CMOS-compatible to biological materials and from electron-beam lithography to R2R processing. These principles have already been applied to a variety of optical components and systems including metasurfaces, sensors, and photonic interconnections, which empower many applications covering integrated imaging systems, chemical sensing, biomedical engineering, and optical communications.

Driven by the growing demands, this dynamic field will actively embrace further challenges that will broaden its implementation and applications. New holistic design methodologies are required to ensure that mechanical and optical functionalities are exploited to the fullest. Integrating new functional materials with novel 3D fabrication methods will further enhance device and system capabilities and performances. We foresee that these new technological advances will ultimately extend photonics, traditionally confined to rigid and planar form factors, into the 3D, soft world and fuel a unique stretch of future opportunities.

AUTHOR INFORMATION

Corresponding Authors

Tian Gu − *Department of Materials Science & Engineering, Massachusetts Institute of Technology, Cambridge, Massachusetts 02139, United States;* orcid.org/0000-0003-3989-6927; Email: gutian@mit.edu

Nanshu Lu − *Department of Aerospace Engineering and Engineering Mechanics, University of Texas at Austin, Austin, Texas 78712, United States;* orcid.org/0000-0002-3595-3851; Email: nanshulu@utexas.edu

Authors

Sarah Geiger − *Department of Materials Science & Engineering, Massachusetts Institute of Technology, Cambridge, Massachusetts 02139, United States*

Jérôme Michon − *Department of Materials Science & Engineering, Massachusetts Institute of Technology, Cambridge, Massachusetts 02139, United States*

Siyi Liu − *Department of Aerospace Engineering and Engineering Mechanics, University of Texas at Austin, Austin, Texas 78712, United States*

Jun Qin − *Department of Materials Science & Engineering, Massachusetts Institute of Technology, Cambridge, Massachusetts 02139, United States*

Jimmy Ni − *Sensors and Electron Devices Directorate, U.S. Army Research Lab, Adelphi, Maryland 20783, United States*

Juejun Hu − *Department of Materials Science & Engineering, Massachusetts Institute of Technology, Cambridge, Massachusetts 02139, United States*

Complete contact information is available at: https://pubs.acs.org/10.1021/acsphotonics.0c00983

Author Contributions

‖S.G., J.M., and S.L. contributed equally to this work.

Notes

The authors declare no competing financial interest.

ACKNOWLEDGMENTS

S.G., J.M., J.Q., J.H., and T.G. acknowledge funding from the National Science Foundation under awards 1453218 and 1506605 and from the DARPA Defense Sciences Office (DSO) Program: EXTREME Optics and Imaging (EXTREME) under agreement no. HR00111720029. N.L. and J.N. acknowledge the support from Army Research Laboratory (ARL) cooperative agreement no. W911NF1820270.

REFERENCES

(1) Reuss, R. H.; Chalamala, B. R.; Moussessian, A.; Kane, M. G.; Kumar, A.; Zhang, D. C.; Rogers, J. A.; Hatalis, M.; Temple, D.; Moddel, G.; Eliasson, B. J.; Estes, M. J.; Kunze, J.; Handy, E. S.; Harmon, E. S.; Salzman, D. B.; Woodall, J. M.; Alam, M. A.; Murthy, J. Y.; Jacobsen, S. C.; Olivier, M.; Markus, D.; Campbell, P. M.; Snow, E. Macroelectronics: Perspectives on Technology and Applications. *Proc. IEEE* **2005**, *93*, 1239−1256.

(2) Bruck, R.; Muellner, P.; Kataeva, N.; Koeck, A.; Trassl, S.; Rinnerbauer, V.; Schmidegg, K.; Hainberger, R. Flexible Thin-Film Polymer Waveguides Fabricated in an Industrial Roll-to-Roll Process. *Appl. Opt.* **2013**, *52* (19), 4510−4514.

(3) Shneidman, A. V.; Becker, K. P.; Lukas, M. A.; Torgerson, N.; Wang, C.; Reshef, O.; Burek, M. J.; Paul, K.; McLellan, J.; Lončar, M. All-Polymer Integrated Optical Resonators by Roll-to-Roll Nanoimprint Lithography. *ACS Photonics* **2018**, *5* (5), 1839−1845.

(4) Ahn, S. H.; Guo, L. J. High-Speed Roll-to-Roll Nanoimprint Lithography on Flexible Plastic Substrates. *Adv. Mater.* **2008**, *20* (11), 2044−2049.

(5) Ok, J. G.; Seok Youn, H.; Kyu Kwak, M.; Lee, K.-T.; Jae Shin, Y.; Jay Guo, L.; Greenwald, A.; Liu, Y. Continuous and Scalable Fabrication of Flexible Metamaterial Films via Roll-to-Roll Nanoimprint Process for Broadband Plasmonic Infrared Filters. *Appl. Phys. Lett.* **2012**, *101* (22), 223102.

(6) Liang, H. L.; Bay, M. M.; Vadrucci, R.; Barty-King, C. H.; Peng, J.; Baumberg, J. J.; De Volder, M. F. L.; Vignolini, S. Roll-to-Roll Fabrication of Touch-Responsive Cellulose Photonic Laminates. *Nat. Commun.* **2018**, *9* (1), 1−7.

(7) Kim, D.-H.; Lu, N.; Ma, R.; Kim, Y.-S.; Kim, R.-H.; Wang, S.; Wu, J.; Won, S. M.; Tao, H.; Islam, A.; Yu, K. J.; Kim, T.; Chowdhury, R.; Ying, M.; Xu, L.; Li, M.; Chung, H.-J.; Keum, H.; McCormick, M.; Liu, P.; Zhang, Y.-W.; Omenetto, F. G.; Huang, Y.; Coleman, T.; Rogers, J. a. Epidermal Electronics. *Science* **2011**, *333* (6044), 838−843.

(8) Gao, W.; Emaminejad, S.; Nyein, H. Y. Y.; Challa, S.; Chen, K.; Peck, A.; Fahad, H. M.; Ota, H.; Shiraki, H.; Kiriya, D.; Lien, D. H.; Brooks, G. A.; Davis, R. W.; Javey, A. Fully Integrated Wearable Sensor Arrays for Multiplexed in Situ Perspiration Analysis. *Nature* **2016**, *529* (7587), 509−514.

(9) Liu, Y.; Pharr, M.; Salvatore, G. A. Lab-on-Skin: A Review of Flexible and Stretchable Electronics for Wearable Health Monitoring. *ACS Nano* **2017**, *11* (10), 9614−9635.
(10) Yu, X.; Xie, Z.; Yu, Y.; Lee, J.; Vazquez-Guardado, A.; Luan, H.; Ruban, J.; Ning, X.; Akhtar, A.; Li, D.; Ji, B.; Liu, Y.; Sun, R.; Cao, J.; Huo, Q.; Zhong, Y.; Lee, C. M.; Kim, S. Y.; Gutruf, P.; Zhang, C.; Xue, Y.; Guo, Q.; Chempakasseril, A.; Tian, P.; Lu, W.; Jeong, J. Y.; Yu, Y. J.; Cornman, J.; Tan, C. S.; Kim, B. H.; Lee, K. H.; Feng, X.; Huang, Y.; Rogers, J. A. Skin-Integrated Wireless Haptic Interfaces for Virtual and Augmented Reality. *Nature* **2019**, *575* (7783), 473−479.
(11) Kim, Y.; Chortos, A.; Xu, W.; Liu, Y.; Oh, J. Y.; Son, D.; Kang, J.; Foudeh, A. M.; Zhu, C.; Lee, Y.; Niu, S.; Liu, J.; Pfattner, R.; Bao, Z.; Lee, T. W. A Bioinspired Flexible Organic Artificial Afferent Nerve. *Science (Washington, DC, U. S.)* **2018**, *360* (6392), 998−1003.
(12) Rogers, J. A.; Someya, T.; Huang, Y. Materials and Mechanics for Stretchable Electronics. *Science* **2010**, *327* (5973), 1603−1607.
(13) Xu, S.; Yan, Z.; Jang, K.-I.; Huang, W.; Fu, H.; Kim, J.; Wei, Z.; Flavin, M.; McCracken, J.; Wang, R.; Badea, A.; Liu, Y.; Xiao, D.; Zhou, G.; Lee, J.; Chung, H. U.; Cheng, H.; Ren, W.; Banks, A.; Li, X.; Paik, U.; Nuzzo, R. G.; Huang, Y.; Zhang, Y.; Rogers, J. A. Assembly of Micro/Nanomaterials into Complex, Three-Dimensional Architectures by Compressive Buckling. *Science (Washington, DC, U. S.)* **2015**, *347* (6218), 154−159.
(14) Bao, Z.; Chen, X. Flexible and Stretchable Devices. *Adv. Mater.* **2016**, *28* (22), 4177−4179.
(15) Wang, S.; Li, M.; Wu, J.; Kim, D. H.; Lu, N.; Su, Y.; Kang, Z.; Huang, Y.; Rogers, J. A. Mechanics of Epidermal Electronics. *J. Appl. Mech.* **2012**, *79* (3), 1.
(16) Sun, Y.; Choi, W. M.; Jiang, H.; Huang, Y. Y.; Rogers, J. A. Controlled Buckling of Semiconductor Nanoribbons for Stretchable Electronics. *Nat. Nanotechnol.* **2006**, *1* (3), 201−207.
(17) Hussain, M. M.; Ma, Z. J.; Shaikh, S. F. Flexible and Stretchable Electronicsprogress,Challenges, and Prospects. *Electrochem. Soc. Interface* **2018**, *27* (4), 65−69.
(18) Verplancke, R.; Bossuyt, F.; Cuypers, D.; Vanfleteren, J. Thin-Film Stretchable Electronics Technology Based on Meandering Interconnections: Fabrication and Mechanical Performance. *J. Micromech. Microeng.* **2012**, *22* (1), 015002.
(19) Khang, D.-Y.; Jiang, H.; Huang, Y.; Rogers, J. A. A Stretchable Form of Single-Crystal Silicon for High-Performance Electronics on Rubber Substrates. *Science* **2006**, *311* (5758), 208−212.
(20) Yuan, H.-C.; Ma, Z.; Roberts, M. M.; Savage, D. E.; Lagally, M. G. High-Speed Strained-Single-Crystal-Silicon Thin-Film Transistors on Flexible Polymers. *J. Appl. Phys.* **2006**, *100* (1), 013708.
(21) Seo, J. H.; Zhang, K.; Kim, M.; Zhao, D.; Yang, H.; Zhou, W.; Ma, Z. Flexible Phototransistors Based on Single-Crystalline Silicon Nanomembranes. *Adv. Opt. Mater.* **2016**, *4* (1), 120−125.
(22) Huang, H. Flexible Wireless Antenna Sensor: A Review. *IEEE Sens. J.* **2013**, *13*, 3865−3872.
(23) Dembo, H.; Kurokawa, Y.; Ikeda, T.; Iwata, S.; Ohshima, K.; Ishii, J.; Tsurume, T.; Sugiyama, E.; Yamada, D.; Isobe, A.; Saito, S.; Dairiki, K.; Kusumoto, N.; Shionoiri, Y.; Atsumi, T.; Fujita, M.; Kobayashi, H.; Takashina, H.; Yamashita, Y.; Yamazaki, S. RFCPUs on Glass and Plastic Substrates Fabricated by TFT Transfer Technology. *IEEE InternationalElectron Devices Meeting, 2005. IEDM Technical Digest* **2005**, 125−127.
(24) Li, N.; Chen, Z.; Ren, W.; Li, F.; Cheng, H.-M. Flexible Graphene-Based Lithium Ion Batteries with Ultrafast Charge and Discharge Rates. *Proc. Natl. Acad. Sci. U. S. A.* **2012**, *109* (43), 17360−17365.
(25) Chen, Z.; To, J. W. F.; Wang, C.; Lu, Z.; Liu, N.; Chortos, A.; Pan, L.; Wei, F.; Cui, Y.; Bao, Z. A Three-Dimensionally Interconnected Carbon Nanotube-Conducting Polymer Hydrogel Network for High-Performance Flexible Battery Electrodes. *Adv. Energy Mater.* **2014**, *4* (12), 1400207.
(26) Park, S.-I.; Xiong, Y.; Kim, R.-H.; Elvikis, P.; Meitl, M.; Kim, D.-H.; Wu, J.; Yoon, J.; Yu, C.-J.; Liu, Z.; Huang, Y.; Hwang, K.; Ferreira, P.; Li, X.; Choquette, K.; Rogers, J. A. Printed Assemblies of Inorganic Light-Emitting Diodes for Deformable and Semitransparent Displays. *Science* **2009**, *325* (5943), 977−981.
(27) Chen, J. Y.; Lau, Y. C.; Coey, J. M. D.; Li, M.; Wang, J. P. High Performance MgO-Barrier Magnetic Tunnel Junctions for Flexible and Wearable Spintronic Applications. *Sci. Rep.* **2017**, *7* (1), 1−7.
(28) Peng, W.; Wu, H. Flexible and Stretchable Photonic Sensors Based on Modulation of Light Transmission. *Adv. Opt. Mater.* **2019**, *7* (12), 1900329.
(29) Walia, S.; Shah, C. M.; Gutruf, P.; Nili, H.; Chowdhury, D. R.; Withayachumnankul, W.; Bhaskaran, M.; Sriram, S. Flexible Metasurfaces and Metamaterials: A Review of Materials and Fabrication Processes at Micro- and Nano-Scales. *Appl. Phys. Rev.* **2015**, *2* (1), 011303.
(30) Lee, G. H.; Moon, H.; Kim, H.; Lee, G. H.; Kwon, W.; Yoo, S.; Myung, D.; Yun, S. H.; Bao, Z.; Hahn, S. K. Multifunctional Materials for Implantable and Wearable Photonic Healthcare Devices. *Nat. Rev. Mater.* **2020**, *5*, 149−165.
(31) Cai, S.; Han, Z.; Wang, F.; Zheng, K.; Cao, Y.; Ma, Y.; Feng, X. Review on Flexible Photonics/Electronics Integrated Devices and Fabrication Strategy. *Sci. China Inf. Sci.* **2018**, *61*, 27.
(32) Ma, H.; Jen, A. K. Y.; Dalton, L. R. Polymer-Based Optical Waveguides: Materials, Processing, and Devices. *Adv. Mater.* **2002**, *14* (19), 1339−1365.
(33) Dangel, R.; La Porta, A.; Jubin, D.; Horst, F.; Meier, N.; Seifried, M.; Offrein, B. J. Polymer Waveguides Enabling Scalable Low-Loss Adiabatic Optical Coupling for Silicon Photonics. *IEEE J. Sel. Top. Quantum Electron.* **2018**, *24* (4), 1.
(34) Huang, Y.; Paloczi, G. T.; Poon, J. K. S.; Yariv, A. Demonstration of Flexible Freestanding All-Polymer Integrated Optical Ring Resonator Devices. *Adv. Mater.* **2004**, *16* (1), 44−48.
(35) Lin, X.; Ling, T.; Subbaraman, H.; Guo, L. J.; Chen, R. T. Printable Thermo-Optic Polymer Switches Utilizing Imprinting and Ink-Jet Printing. *Opt. Express* **2013**, *21* (2), 2110.
(36) Song, H. C.; Oh, M. C.; Ahn, S. W.; Steier, W. H.; Fetterman, H. R.; Zhang, C. Flexible Low-Voltage Electro-Optic Polymer Modulators. *Appl. Phys. Lett.* **2003**, *82* (25), 4432−4434.
(37) Choi, C.; Lin, L.; Liu, Y.; Choi, J.; Wang, L.; Haas, D.; Magera, J.; Chen, R. T. Flexible Optical Waveguide Film Fabrications and Optoelectronic Devices Integration for Fully Embedded Board-Level Optical Interconnects. *J. Lightwave Technol.* **2004**, *22* (9), 2168−2176.
(38) Bhola, B.; Song, H.-C.; Tazawa, H.; Steier, W. H. Polymer Microresonator Strain Sensors. *IEEE Photonics Technol. Lett.* **2005**, *17* (4), 867−869.
(39) Kim, K.-J.; Seo, J.-K.; Oh, M.-C. Strain Induced Tunable Wavelength Filters Based on Flexible Polymer Waveguide Bragg Reflector. *Opt. Express* **2008**, *16* (3), 1423.
(40) Li, R.-Z.; Zhang, L.-J.; Hu, W.; Wang, L.-D.; Tang, J.; Zhang, T. Flexible TE-Pass Polymer Waveguide Polarizer with Low Bending Loss. *IEEE Photonics Technol. Lett.* **2016**, *28* (22), 2601−2604.
(41) Maeda, Y.; Hashiguchi, Y. Flexible Film Waveguides with Excellent Bending Properties. *Proc. SPIE* **2008**, *6899*, 68990D.
(42) Missinne, J.; Van Steenberge, G.; Van Hoe, B.; Van Coillie, K.; Van Gijseghem, T.; Dubruel, P.; Vanfleteren, J.; Van Daele, P. An Array Waveguide Sensor for Artificial Optical Skins. *Proc. SPIE* **2009**, *7221*, 722105.
(43) Kinoshita, R.; Suganuma, D.; Ishigure, T. Accurate Interchannel Pitch Control in Graded-Index Circular-Core Polymer Parallel Optical Waveguide Using the Mosquito Method. *Opt. Express* **2014**, *22* (7), 8426.
(44) Cai, D. K.; Neyer, A. Polysiloxane Based Flexible Electrical-Optical-Circuits-Board. *Microelectron. Eng.* **2010**, *87* (11), 2268−2274.
(45) To, C.; Hellebrekers, T.; Jung, J.; Yoon, S. J.; Park, Y. L. A Soft Optical Waveguide Coupled with Fiber Optics for Dynamic Pressure and Strain Sensing. *IEEE Robot. Autom. Lett.* **2018**, *3* (4), 3821−3827.
(46) Rubehn, B.; Wolff, S. B. E.; Tovote, P.; Lüthi, A.; Stieglitz, T. A Polymer-Based Neural Microimplant for Optogenetic Applications: Design and First in Vivo Study. *Lab Chip* **2013**, *13* (4), 579−588.

https://dx.doi.org/10.1021/acsphotonics.0c00983
ACS Photonics XXXX, XXX, XXX−XXX

(47) Lostutter, C. K.; Hodge, M. H.; Marrapode, T. R.; Swatowski, B. W.; Weidner, W. K. Assembly and Performance of Silicone Polymer Waveguides. *Proc. SPIE* **2016**, *9753*, 97530K.
(48) John, R. S. E.; Amb, C. M.; Swatowski, B. W.; Weidner, W. K.; Halter, M.; Lamprecht, T.; Betschon, F. Thermally Stable, Low Loss Optical Silicones: A Key Enabler for Electro-Optical Printed Circuit Boards. *J. Lightwave Technol.* **2015**, *33* (4), 814−819.
(49) Reddy, J. W.; Chamanzar, M. Low-Loss Flexible Parylene Photonic Waveguides for Optical Implants. *Opt. Lett.* **2018**, *43* (17), 4112.
(50) Yang, J.; Zhou, Q.; Chen, R. T. Polyimide-Waveguide-Based Thermal Optical Switch Using Total-Internal- Reflection Effect. *Appl. Phys. Lett.* **2002**, *81* (16), 2947−2949.
(51) Khan, M. U.; McGrath, J.; Corbett, B.; Pemble, M. Air-Clad Broadband Waveguide Using Micro-Molded Polyimide Combined with a Robust, Silica-Based Inverted Opal Substrate. *Opt. Mater. Express* **2017**, *7* (9), 3155.
(52) Buestrich, R.; Kahlenberg, F.; Popall, M.; Dannberg, P.; Müller-Fiedler, R.; Rösch, O. ORMOCERs for Optical Interconnection Technology. *J. Sol-Gel Sci. Technol.* **2001**, *20* (2), 181−186.
(53) Girschikofsky, M.; Förthner, M.; Rommel, M.; Frey, L.; Hellmann, R. Waveguide Bragg Gratings in Ormocer Hybrid Polymers. *Opt. Express* **2016**, *24* (13), 14725.
(54) Zuo, H.; Yu, S.; Gu, T.; Hu, J. Low Loss, Flexible Single-Mode Polymer Photonics. *Opt. Express* **2019**, *27* (8), 11152.
(55) Dougherty, T. J.; Gomer, C. J.; Henderson, B. W.; Jori, G.; Kessel, D.; Korbelik, M.; Moan, J.; Peng, Q. Photodynamic Therapy. *JNCI J. Natl. Cancer Inst.* **1998**, *90* (12), 889−905.
(56) Toettcher, J. E.; Gong, D.; Lim, W. A.; Weiner, O. D. Light-Based Feedback for Controlling Intracellular Signaling Dynamics. *Nat. Methods* **2011**, *8* (10), 837−839.
(57) Yun, S. H.; Kwok, S. J. J. Light in Diagnosis, Therapy and Surgery. *Nat. Biomed. Eng.* **2017**, *1* (1), 1−16.
(58) Fenno, L.; Yizhar, O.; Deisseroth, K. The Development and Application of Optogenetics. *Annu. Rev. Neurosci.* **2011**, *34* (1), 389−412.
(59) Shabahang, S.; Kim, S.; Yun, S. H. Light-Guiding Biomaterials for Biomedical Applications. *Adv. Funct. Mater.* **2018**, *28* (24), 1706635.
(60) Choi, M.; Choi, J. W.; Kim, S.; Nizamoglu, S.; Hahn, S. K.; Yun, S. H. Light-Guiding Hydrogels for Cell-Based Sensing and Optogenetic Synthesis in Vivo. *Nat. Photonics* **2013**, *7* (12), 987−994.
(61) Nizamoglu, S.; Gather, M. C.; Humar, M.; Choi, M.; Kim, S.; Kim, K. S.; Hahn, S. K.; Scarcelli, G.; Randolph, M.; Redmond, R. W.; Yun, S. H. Bioabsorbable Polymer Optical Waveguides for Deep-Tissue Photomedicine. *Nat. Commun.* **2016**, *7* (1), 1−7.
(62) Xu, H.; Yin, L.; Liu, C.; Sheng, X.; Zhao, N. Recent Advances in Biointegrated Optoelectronic Devices. *Adv. Mater.* **2018**, *30*, 1800156.
(63) Qiao, X.; Qian, Z.; Li, J.; Sun, H.; Han, Y.; Xia, X.; Zhou, J.; Wang, C.; Wang, Y.; Wang, C. Synthetic Engineering of Spider Silk Fiber as Implantable Optical Waveguides for Low-Loss Light Guiding. *ACS Appl. Mater. Interfaces* **2017**, *9* (17), 14665−14676.
(64) Xu, L.; Jiang, X.; Zhao, G.; Ma, D.; Tao, H.; Liu, Z.; Omenetto, F. G.; Yang, L. High-Q Silk Fibroin Whispering Gallery Microresonator. *Opt. Express* **2016**, *24* (18), 20825.
(65) Applegate, M. B.; Perotto, G.; Kaplan, D. L.; Omenetto, F. G. Biocompatible Silk Step-Index Optical Waveguides. *Biomed. Opt. Express* **2015**, *6* (11), 4221.
(66) Frka-Petesic, B.; Vignolini, S. So Much More than Paper. *Nat. Photonics* **2019**, *13*, 365−367.
(67) Guidetti, G.; Atifi, S.; Vignolini, S.; Hamad, W. Y. Flexible Photonic Cellulose Nanocrystal Films. *Adv. Mater.* **2016**, *28* (45), 10042−10047.
(68) Manocchi, A. K.; Domachuk, P.; Omenetto, F. G.; Yi, H. Facile Fabrication of Gelatin-Based Biopolymeric Optical Waveguides. *Biotechnol. Bioeng.* **2009**, *103* (4), 725−732.
(69) Kharkar, P. M.; Kiick, K. L.; Kloxin, A. M. Designing Degradable Hydrogels for Orthogonal Control of Cell Microenvironments. *Chem. Soc. Rev.* **2013**, *42* (17), 7335−7372.
(70) Khetan, S.; Guvendiren, M.; Legant, W. R.; Cohen, D. M.; Chen, C. S.; Burdick, J. A. Degradation-Mediated Cellular Traction Directs Stem Cell Fate in Covalently Crosslinked Three-Dimensional Hydrogels. *Nat. Mater.* **2013**, *12* (5), 458−465.
(71) Caliari, S. R.; Burdick, J. A. A Practical Guide to Hydrogels for Cell Culture. *Nat. Methods* **2016**, *13*, 405−414.
(72) Omenetto, F. G.; Kaplan, D. L. A New Route for Silk. *Nat. Photonics* **2008**, *2* (11), 641−643.
(73) Omenetto, F. G.; Kaplan, D. L. New Opportunities for an Ancient Material. *Science (Washington, DC, U. S.)* **2010**, *329* (5991), 528−531.
(74) Applegate, M. B.; Brenckle, M. A.; Marelli, B.; Tao, H.; Kaplan, D. L.; Omenetto, F. G. Silk: A Different Kind of "Fiber Optics. *Opt. Photonics News* **2014**, *25* (6), 28.
(75) Kujala, S.; Mannila, A.; Karvonen, L.; Kieu, K.; Sun, Z. Natural Silk as a Photonics Component: A Study on Its Light Guiding and Nonlinear Optical Properties. *Sci. Rep.* **2016**, *6* (1), 1−9.
(76) Jain, A.; Yang, A. H. J.; Erickson, D. Gel-Based Optical Waveguides with Live Cell Encapsulation and Integrated Microfluidics. *Opt. Lett.* **2012**, *37* (9), 1472.
(77) Parker, S. T.; Domachuk, P.; Amsden, J.; Bressner, J.; Lewis, J. A.; Kaplan, D. L.; Omenetto, F. C. Biocompatible Silk Printed Optical Waveguides. *Adv. Mater.* **2009**, *21* (23), 2411−2415.
(78) Chen, Y.; Li, H.; Li, M. Flexible and Tunable Silicon Photonic Circuits on Plastic Substrates. *Sci. Rep.* **2012**, *2*, 622.
(79) Fan, L.; Varghese, L. T.; Xuan, Y.; Wang, J.; Niu, B.; Qi, M. Direct Fabrication of Silicon Photonic Devices on a Flexible Platform and Its Application for Strain Sensing. *Opt. Express* **2012**, *20* (18), 20564−20575.
(80) Cavallo, F.; Lagally, M. G. Semiconductors Turn Soft: Inorganic Nanomembranes. *Soft Matter* **2010**, *6* (3), 439−455.
(81) Aksu, S.; Huang, M.; Artar, A.; Yanik, A. A.; Selvarasah, S.; Dokmeci, M. R.; Altug, H. Flexible Plasmonics on Unconventional and Nonplanar Substrates. *Adv. Mater.* **2011**, *23* (38), 4422−4430.
(82) Ee, H. S.; Agarwal, R. Tunable Metasurface and Flat Optical Zoom Lens on a Stretchable Substrate. *Nano Lett.* **2016**, *16* (4), 2818−2823.
(83) Liu, X.; Wang, J.; Tang, L.; Xie, L.; Ying, Y. Flexible Plasmonic Metasurfaces with User-Designed Patterns for Molecular Sensing and Cryptography. *Adv. Funct. Mater.* **2016**, *26* (30), 5515−5523.
(84) Gong, S.; Schwalb, W.; Wang, Y.; Chen, Y.; Tang, Y.; Si, J.; Shirinzadeh, B.; Cheng, W. A Wearable and Highly Sensitive Pressure Sensor with Ultrathin Gold Nanowires. *Nat. Commun.* **2014**, *5* (1), 1−8.
(85) Li, L.; Lin, H.; Michon, J.; Huang, Y.; Li, J.; Du, Q.; Yadav, A.; Richardson, K.; Gu, T.; Hu, J. A New Twist on Glass: A Brittle Material Enabling Flexible Integrated Photonics. *Int. J. Appl. Glas. Sci.* **2017**, *8* (1), 61−68.
(86) Lapointe, J.; Ledemi, Y.; Loranger, S.; Iezzi, V. L.; Soares de Lima Filho, E.; Parent, F.; Morency, S.; Messaddeq, Y.; Kashyap, R. Fabrication of Ultrafast Laser Written Low-Loss Waveguides in Flexible As2S3 Chalcogenide Glass Tape. *Opt. Lett.* **2016**, *41* (2), 203−206.
(87) Zou, Y.; Zhang, D.; Lin, H.; Li, L.; Moreel, L.; Zhou, J.; Du, Q.; Ogbuu, O.; Danto, S.; Musgraves, J. D.; Richardson, K.; Dobson, K. D.; Birkmire, R.; Hu, J. High-Performance, High-Index-Contrast Chalcogenide Glass Photonics on Silicon and Unconventional Non-Planar Substrates. *Adv. Opt. Mater.* **2014**, *2*, 478−486.
(88) Zou, Y.; Moreel, L.; Lin, H.; Zhou, J.; Li, L.; Danto, S.; Musgraves, J. D.; Koontz, E.; Richardson, K.; Dobson, K. D.; Birkmire, R.; Hu, J. Solution Processing and Resist-Free Nanoimprint Fabrication of Thin Film Chalcogenide Glass Devices: Inorganic-Organic Hybrid Photonic Integration. *Adv. Opt. Mater.* **2014**, *2* (8), 759−764.
(89) Hu, J.; Li, L.; Lin, H.; Zou, Y.; Du, Q.; Smith, C.; Novak, S.; Richardson, K.; Musgraves, J. D. Chalcogenide Glass Microphotonics:

https://dx.doi.org/10.1021/acsphotonics.0c00983
ACS Photonics XXXX, XXX, XXX−XXX

Stepping into the Spotlight. *Am. Ceram. Soc. Bull.* **2015**, *94* (4), 24−29.
(90) Yu, K. J.; Yan, Z.; Han, M.; Rogers, J. A. Inorganic Semiconducting Materials for Flexible and Stretchable Electronics. *npj Flex. Electron.* **2017**, *1* (1), 1−14.
(91) Rogers, J. A.; Lagally, M. G.; Nuzzo, R. G. Synthesis, Assembly and Applications of Semiconductor Nanomembranes. *Nature* **2011**, *477* (7362), 45−53.
(92) Zhou, W.; Ma, Z.; Yang, W.; Chuwongin, S.; Shuai, Y.-C.; Seo, J.-H.; Zhao, D.; Yang, H.; Soref, R. Semiconductor Nanomembranes for Integrated and Flexible Photonics. *2011 ICO International Conference on Information Photonics* **2011**, 1−2.
(93) Lin, H.; Song, Y.; Huang, Y.; Kita, D.; Deckoff-Jones, S.; Wang, K.; Li, L.; Li, J.; Zheng, H.; Luo, Z.; Wang, H.; Novak, S.; Yadav, A.; Huang, C.-C.; Shiue, R.-J.; Englund, D.; Gu, T.; Hewak, D.; Richardson, K.; Kong, J.; Hu, J. Chalcogenide Glass-on-Graphene Photonics. *Nat. Photonics* **2017**, *11* (12), 798−805.
(94) Choi, C.; Lee, Y.; Cho, K. W.; Koo, J. H.; Kim, D. H. Wearable and Implantable Soft Bioelectronics Using Two-Dimensional Materials. *Acc. Chem. Res.* **2019**, *52* (1), 73−81.
(95) Shi, Y.; Rogers, J. A.; Gao, C.; Huang, Y. Multiple Neutral Axes in Bending of a Multiple-Layer Beam with Extremely Different Elastic Properties. *J. Appl. Mech.* **2014**, *81* (11), 4028465.
(96) Hu, J.; Li, L.; Lin, H.; Zhang, P.; Zhou, W.; Ma, Z. Flexible Integrated Photonics: Where Materials, Mechanics and Optics Meet [Invited]. *Opt. Mater. Express* **2013**, *3* (9), 1313.
(97) Li, L.; Lin, H.; Qiao, S.; Zou, Y.; Danto, S.; Richardson, K.; Musgraves, J. D.; Lu, N.; Hu, J. Integrated Flexible Chalcogenide Glass Photonic Devices. *Nat. Photonics* **2014**, *8* (8), 643−649.
(98) Li, L.; Zhang, P.; Wang, W.-M.; Lin, H.; Zerdoum, A. B.; Geiger, S. J.; Liu, Y.; Xiao, N.; Zou, Y.; Ogbuu, O.; Du, Q.; Jia, X.; Li, J.; Hu, J. Foldable and Cytocompatible Sol-Gel TiO2 Photonics. *Sci. Rep.* **2015**, *5*, 13832.
(99) Li, L.; Lin, H.; Huang, Y.; Shiue, R.-J.; Yadav, A.; Li, J.; Michon, J.; Englund, D.; Richardson, K.; Gu, T.; Hu, J. High-Performance Flexible Waveguide-Integrated Photodetectors. *Optica* **2018**, *5* (1), 44.
(100) Missinne, J.; Kalathimekkad, S.; Van Hoe, B.; Bosman, E.; Vanfleteren, J.; Van Steenberge, G. Stretchable Optical Waveguides. *Opt. Express* **2014**, *22* (4), 4168−4179.
(101) Li, L.; Lin, H.; Qiao, S.; Huang, Y.-Z.; Li, J.-Y.; Michon, J.; Gu, T.; Alosno-Ramos, C.; Vivien, L.; Yadav, A.; Richardson, K.; Lu, N.; Hu, J. Monolithically Integrated Stretchable Photonics. *Light: Sci. Appl.* **2018**, *7* (2), 17138.
(102) Kamali, S. M.; Arbabi, A.; Arbabi, E.; Horie, Y.; Faraon, A. Decoupling Optical Function and Geometrical Form Using Conformal Flexible Dielectric Metasurfaces. *Nat. Commun.* **2016**, *7* (1), 11618.
(103) Kamali, S. M.; Arbabi, E.; Arbabi, A.; Horie, Y.; Faraon, A. Highly Tunable Elastic Dielectric Metasurface Lenses. *Laser Photonics Rev.* **2016**, *10* (6), 1002−1008.
(104) Yu, C. L.; Kim, H.; De Leon, N.; Frank, I. W.; Robinson, J. T.; McCutcheon, M.; Liu, M.; Lukin, M. D.; Loncar, M.; Park, H. Stretchable Photonic Crystal Cavity with Wide Frequency Tunability. *Nano Lett.* **2013**, *13* (1), 248−252.
(105) Lin, H. I.; Shen, K. C.; Lin, S. Y.; Haider, G.; Li, Y. H.; Chang, S. W.; Chen, Y. F. Transient and Flexible Hyperbolic Metamaterials on Freeform Surfaces. *Sci. Rep.* **2018**, *8* (1), 1−10.
(106) Capper, P.; Irvine, S.; Joyce, T. Epitaxial Crystal Growth: Methods and Materials. *Springer Handbook of Electronic and Photonic Materials* **2017**, 1.
(107) Ma, Z.; Liu, D. *Inorganic Flexible Optoelectronics*; Wiley, 2019.
(108) Kum, H.; Lee, D.; Kong, W.; Kim, H.; Park, Y.; Kim, Y.; Baek, Y.; Bae, S. H.; Lee, K.; Kim, J. Epitaxial Growth and Layer-Transfer Techniques for Heterogeneous Integration of Materials for Electronic and Photonic Devices. *Nat. Electron.* **2019**, *2* (10), 439−450.
(109) Vasudev, A. P.; Kang, J.-H.; Park, J.; Liu, X.; Brongersma, M. L. Electro-Optical Modulation of a Silicon Waveguide with an "Epsilon-near-Zero" Material. *Opt. Express* **2013**, *21* (22), 26387.
(110) Kinsey, N.; DeVault, C.; Kim, J.; Ferrera, M.; Shalaev, V. M.; Boltasseva, A. Epsilon-near-Zero Al-Doped ZnO for Ultrafast Switching at Telecom Wavelengths. *Optica* **2015**, *2* (7), 616.
(111) Rensberg, J.; Zhou, Y.; Richter, S.; Wan, C.; Zhang, S.; Schöppe, P.; Schmidt-Grund, R.; Ramanathan, S.; Capasso, F.; Kats, M. A.; Ronning, C. Epsilon-Near-Zero Substrate Engineering for Ultrathin-Film Perfect Absorbers. *Phys. Rev. Appl.* **2017**, *8* (1), 014009.
(112) Ni, J. H.; Sarney, W. L.; Leff, A. C.; Cahill, J. P.; Zhou, W. Property Variation in Wavelength-Thick Epsilon-Near-Zero ITO Metafilm for Near IR Photonic Devices. *Sci. Rep.* **2020**, *10* (1), 1−8.
(113) Ghaffari, A.; Hosseini, A.; Xu, X.; Kwong, D.; Subbaraman, H.; Chen, R. T. Transfer of Micro and Nano-Photonic Silicon Nanomembrane Waveguide Devices on Flexible Substrates. *Opt. Express* **2010**, *18* (19), 20086−20095.
(114) Xu, X.; Subbaraman, H.; Pham, D. T.; Hosseini, A.; Ghaffari, A.; Chen, R. T. Flexible In-Plane Photonic Devices Based on Transferrable Si Nanomembranes on Polyimide Film. *J. Phys. Conf. Ser.* **2011**, *276* (1), 012096.
(115) Yuan, H.-C.; Shin, J.; Qin, G.; Sun, L.; Bhattacharya, P.; Lagally, M. G.; Celler, G. K.; Ma, Z. Flexible Photodetectors on Plastic Substrates by Use of Printing Transferred Single-Crystal Germanium Membranes. *Appl. Phys. Lett.* **2009**, *94* (1), 013102.
(116) Yang, W.; Yang, H.; Qin, G.; Ma, Z.; Berggren, J.; Hammar, M.; Soref, R.; Zhou, W. Large-Area InP-Based Crystalline Nanomembrane Flexible Photodetectors. *Appl. Phys. Lett.* **2010**, *96* (12), 121107.
(117) Gissibl, T.; Thiele, S.; Herkommer, A.; Giessen, H. Two-Photon Direct Laser Writing of Ultracompact Multi-Lens Objectives. *Nat. Photonics* **2016**, *10* (8), 554−560.
(118) Corbett, B.; Loi, R.; Zhou, W.; Liu, D.; Ma, Z. Transfer Print Techniques for Heterogeneous Integration of Photonic Components. *Prog. Quantum Electron.* **2017**, *52*, 1−17.
(119) Chen, Y.; Li, M. Integrated Silicon and Silicon Nitride Photonic Circuits on Flexible Substrates. *Opt. Lett.* **2014**, *39* (12), 3449.
(120) Xu, X.; Subbaraman, H.; Hosseini, A.; Lin, C.-Y.; Kwong, D.; Chen, R. T. Stamp Printing of Silicon-Nanomembrane-Based Photonic Devices onto Flexible Substrates with a Suspended Configuration. *Opt. Lett.* **2012**, *37* (6), 1020.
(121) Meitl, M. A.; Zhu, Z.-T.; Kumar, V.; Lee, K. J.; Feng, X.; Huang, Y. Y.; Adesida, I.; Nuzzo, R. G.; Rogers, J. A. Transfer Printing by Kinetic Control of Adhesion to an Elastomeric Stamp. *Nat. Mater.* **2006**, *5* (1), 33−38.
(122) Vernoux, C.; Chen, Y.; Markey, L.; Spârchez, C.; Arocas, J.; Felder, T.; Neitz, M.; Brusberg, L.; Weeber, J.-C.; Bozhevolnyi, S. I.; Dereux, A. Flexible Long-Range Surface Plasmon Polariton Single-Mode Waveguide for Optical Interconnects. *Opt. Mater. Express* **2018**, *8* (2), 469.
(123) Aksu, S.; Yanik, A. A.; Adato, R.; Artar, A.; Huang, M.; Altug, H. High-Throughput Nanofabrication of Infrared Plasmonic Nano-antenna Arrays for Vibrational Nanospectroscopy. *Nano Lett.* **2010**, *10* (7), 2511−2518.
(124) Jain, T.; Aernecke, M.; Liberman, V.; Karnik, R. High Resolution Fabrication of Nanostructures Using Controlled Proximity Nanostencil Lithography. *Appl. Phys. Lett.* **2014**, *104* (8), 083117.
(125) Vazquez-Mena, O.; Gross, L.; Xie, S.; Villanueva, L. G.; Brugger, J. Resistless Nanofabrication by Stencil Lithography: A Review. *Microelectron. Eng.* **2015**, *132*, 236−254.
(126) Zhang, C.; Zou, C.-L.; Zhao, Y.; Dong, C.-H.; Wei, C.; Wang, H.; Liu, Y.; Guo, G.-C.; Yao, J.; Zhao, Y. S. Organic Printed Photonics: From Microring Lasers to Integrated Circuits. *Sci. Adv.* **2015**, *1* (8), e1500257.
(127) Zhou, Y.; Layani, M.; Wang, S.; Hu, P.; Ke, Y.; Magdassi, S.; Long, Y. Fully Printed Flexible Smart Hybrid Hydrogels. *Adv. Funct. Mater.* **2018**, *28* (9), 1705365.
(128) Huang, S.; Li, M.; Garner, S. M.; Li, M.-J.; Chen, K. P. Flexible Photonic Components in Glass Substrates. *Opt. Express* **2015**, *23* (17), 22532.

https://dx.doi.org/10.1021/acsphotonics.0c00983
ACS Photonics XXXX, XXX, XXX−XXX

(129) Sun, Y. L.; Dong, W. F.; Niu, L. G.; Jiang, T.; Liu, D. X.; Zhang, L.; Wang, Y. S.; Chen, Q. D.; Kim, D. P.; Sun, H. B. Protein-Based Soft Micro-Optics Fabricated by Femtosecond Laser Direct Writing. *Light: Sci. Appl.* **2014**, *3* (1), e129−e129.
(130) Muth, J. T.; Vogt, D. M.; Truby, R. L.; Mengüç, Y.; Kolesky, D. B.; Wood, R. J.; Lewis, J. A. Embedded 3D Printing of Strain Sensors within Highly Stretchable Elastomers. *Adv. Mater.* **2014**, *26* (36), 6307−6312.
(131) Cai, D. K.; Neyer, A. Realization of KaptonTM Based Optical Interconnect by KMnO4 Wet Etching. *Appl. Phys. A: Mater. Sci. Process.* **2010**, *99* (4), 783−789.
(132) Choi, M.; Humar, M.; Kim, S.; Yun, S. H. Step-Index Optical Fiber Made of Biocompatible Hydrogels. *Adv. Mater.* **2015**, *27* (27), 4081−4086.
(133) Morarescu, R.; Pal, P. K.; Beneitez, N. T.; Missinne, J.; Steenberge, G. V.; Bienstman, P.; Morthier, G. Fabrication and Characterization of High-Optical-Quality-Factor Hybrid Polymer Microring Resonators Operating at Very Near Infrared Wavelengths. *IEEE Photonics J.* **2016**, *8* (2), 1.
(134) Chanda, D.; Shigeta, K.; Gupta, S.; Cain, T.; Carlson, A.; Mihi, A.; Baca, A. J.; Bogart, G. R.; Braun, P.; Rogers, J. A. Large-Area Flexible 3D Optical Negative Index Metamaterial Formed by Nanotransfer Printing. *Nat. Nanotechnol.* **2011**, *6* (7), 402−407.
(135) Aikio, S.; Hiltunen, J.; Hiitola-Keinänen, J.; Hiltunen, M.; Kontturi, V.; Siitonen, S.; Puustinen, J.; Karioja, P. Disposable Photonic Integrated Circuits for Evanescent Wave Sensors by Ultra-High Volume Roll-to-Roll Method. *Opt. Express* **2016**, *24* (3), 2527.
(136) Teo, J. Y. H.; Wong, L. J.; Molardi, C.; Genevet, P. Controlling Electromagnetic Fields at Boundaries of Arbitrary Geometries. *Phys. Rev. A: At., Mol., Opt. Phys.* **2016**, *94* (2), 023820.
(137) Ni, X.; Wong, Z. J.; Mrejen, M.; Wang, Y.; Zhang, X. An Ultrathin Invisibility Skin Cloak for Visible Light. *Science (Washington, DC, U. S.)* **2015**, *349* (6254), 1310−1314.
(138) Ergin, T.; Stenger, N.; Brenner, P.; Pendry, J. B.; Wegener, M. Three-Dimensional Invisibility Cloak at Optical Wavelengths. *Science (Washington, DC, U. S.)* **2010**, *328* (5976), 337−339.
(139) Tao, H.; Landy, N. I.; Fan, K.; Strikwerda, A. C.; Padilla, W. J.; Averitt, R. D.; Zhang, X. Flexible Terahertz Metamaterials: Towards a Terahertz Metamaterial Invisible Cloak. *2008 IEEE International Electron Devices Meeting* **2008**, 1−4.
(140) Iwaszczuk, K.; Strikwerda, A. C.; Fan, K.; Zhang, X.; Averitt, R. D.; Jepsen, P. U. Flexible Metamaterial Absorbers for Stealth Applications at Terahertz Frequencies. *Opt. Express* **2012**, *20* (1), 635.
(141) Valentine, J.; Li, J.; Zentgraf, T.; Bartal, G.; Zhang, X. An Optical Cloak Made of Dielectrics. *Nat. Mater.* **2009**, *8* (7), 568−571.
(142) Liu, X.; MacNaughton, S.; Shrekenhamer, D. B.; Tao, H.; Selvarasah, S.; Totachawattana, A.; Averitt, R. D.; Dokmeci, M. R.; Sonkusale, S.; Padilla, W. J. Metamaterials on Parylene Thin Film Substrates: Design, Fabrication, and Characterization at Terahertz Frequency. *Appl. Phys. Lett.* **2010**, *96* (1), 011906.
(143) Xu, X.; Peng, B.; Li, D.; Zhang, J.; Wong, L. M.; Zhang, Q.; Wang, S.; Xiong, Q. Flexible Visible-Infrared Metamaterials and Their Applications in Highly Sensitive Chemical and Biological Sensing. *Nano Lett.* **2011**, *11* (8), 3232−3238.
(144) Wen, X.; Li, G.; Zhang, J.; Zhang, Q.; Peng, B.; Wong, L. M.; Wang, S.; Xiong, Q. Transparent Free-Standing Metamaterials and Their Applications in Surface-Enhanced Raman Scattering. *Nanoscale* **2014**, *6* (1), 132−139.
(145) Zhang, G.; Lan, C.; Bian, H.; Gao, R.; Zhou, J. Flexible, All-Dielectric Metasurface Fabricated via Nanosphere Lithography and Its Applications in Sensing. *Opt. Express* **2017**, *25* (18), 22038.
(146) Jiang, Z. H.; Kang, L.; Werner, D. H. Conformal Metasurface-Coated Dielectric Waveguides for Highly Confined Broadband Optical Activity with Simultaneous Low-Visibility and Reduced Crosstalk. *Nat. Commun.* **2017**, *8* (1), 1−10.
(147) Linghu, C.; Zhang, S.; Wang, C.; Song, J. Transfer Printing Techniques for Flexible and Stretchable Inorganic Electronics. *npj Flex. Electron.* **2018**, *2* (1), 1−14.
(148) Le Borgne, B.; De Sagazan, O.; Crand, S.; Jacques, E.; Harnois, M. Conformal Electronics Wrapped Around Daily Life Objects Using an Original Method: Water Transfer Printing. *ACS Appl. Mater. Interfaces* **2017**, *9* (35), 29424−29429.
(149) Sim, K.; Chen, S.; Li, Z.; Rao, Z.; Liu, J.; Lu, Y.; Jang, S.; Ershad, F.; Chen, J.; Xiao, J.; Yu, C. Three-Dimensional Curvy Electronics Created Using Conformal Additive Stamp Printing. *Nat. Electron.* **2019**, *2* (10), 471−479.
(150) Choi, C.; Choi, M. K.; Liu, S.; Kim, M. S.; Park, O. K.; Im, C.; Kim, J.; Qin, X.; Lee, G. J.; Cho, K. W.; Kim, M.; Joh, E.; Lee, J.; Son, D.; Kwon, S. H.; Jeon, N. L.; Song, Y. M.; Lu, N.; Kim, D. H. Human Eye-Inspired Soft Optoelectronic Device Using High-Density MoS2-Graphene Curved Image Sensor Array. *Nat. Commun.* **2017**, *8* (1), 1−11.
(151) Lee, Y. K.; Xi, Z.; Lee, Y. J.; Kim, Y. H.; Hao, Y.; Choi, H.; Lee, M. G.; Joo, Y. C.; Kim, C.; Lien, J. M.; Choi, I. S. Computational Wrapping: A Universal Method to Wrap 3D-Curved Surfaces with Nonstretchable Materials for Conformal Devices. *Sci. Adv.* **2020**, *6* (15), eaax6212.
(152) Zhang, K.; Jung, Y. H.; Mikael, S.; Seo, J. H.; Kim, M.; Mi, H.; Zhou, H.; Xia, Z.; Zhou, W.; Gong, S.; Ma, Z. Origami Silicon Optoelectronics for Hemispherical Electronic Eye Systems. *Nat. Commun.* **2017**, *8* (1), 1−8.
(153) Qiao, S.; Gratadour, J. B.; Wang, L.; Lu, N. Conformability of a Thin Elastic Membrane Laminated on a Rigid Substrate With Corrugated Surface. *IEEE Trans. Compon., Packag., Manuf. Technol.* **2015**, *5* (9), 1237−1243.
(154) Wang, L.; Lu, N. Conformability of a Thin Elastic Membrane Laminated on a Soft Substrate with Slightly Wavy Surface. *J. Appl. Mech.* **2016**, *83* (4), 041007.
(155) Shannon, R. R. Overview of Conformal Optics. *Proc. SPIE* **1999**, *3705*, 180−188.
(156) Yu, N.; Genevet, P.; Kats, M. A.; Aieta, F.; Tetienne, J. P.; Capasso, F.; Gaburro, Z. Light Propagation with Phase Discontinuities: Generalized Laws of Reflection and Refraction. *Science (Washington, DC, U. S.)* **2011**, *334* (6054), 333−337.
(157) Zhang, L.; Ding, J.; Zheng, H.; An, S.; Lin, H.; Zheng, B.; Du, Q.; Yin, G.; Michon, J.; Zhang, Y.; Fang, Z.; Shalaginov, M. Y.; Deng, L.; Gu, T.; Zhang, H.; Hu, J. Ultra-Thin High-Efficiency Mid-Infrared Transmissive Huygens Meta-Optics. *Nat. Commun.* **2018**, *9* (1), 1481.
(158) Agrell, E.; Karlsson, M.; Chraplyvy, A. R.; Richardson, D. J.; Krummrich, P. M.; Winzer, P.; Roberts, K.; Fischer, J. K.; Savory, S. J.; Eggleton, B. J.; Secondini, M.; Kschischang, F. R.; Lord, A.; Prat, J.; Tomkos, I.; Bowers, J. E.; Srinivasan, S.; Brandt-Pearce, M.; Gisin, N. Roadmap of Optical Communications. *J. Opt.* **2016**, *18* (6), 063002.
(159) Yoo, S. J. B. The Role of Photonics in Future Computing and Data Centers. *IEICE Trans. Commun.* **2014**, *E97.B*, 1272−1280.
(160) Miller, D. A. B. Device Requirements for Optical Interconnects to Silicon Chips. *Proc. IEEE* **2009**, *97* (7), 1166−1185.
(161) Gu, T.; Nair, R.; Haney, M. W. Chip-Level Multiple Quantum Well Modulator-Based Optical Interconnects. *J. Lightwave Technol.* **2013**, *31* (24), 4166−4174.
(162) Li, L.; Zou, Y.; Lin, H.; Hu, J.; Sun, X.; Feng, N. N.; Danto, S.; Richardson, K.; Gu, T.; Haney, M. A Fully-Integrated Flexible Photonic Platform for Chip-to-Chip Optical Interconnects. *J. Lightwave Technol.* **2013**, *31* (24), 4080−4086.
(163) Dangel, R.; Horst, F.; Jubin, D.; Meier, N.; Weiss, J.; Offrein, B. J.; Swatowski, B. W.; Amb, C. M.; Deshazer, D. J.; Weidner, W. K. Development of Versatile Polymer Waveguide Flex Technology for Use in Optical Interconnects. *J. Lightwave Technol.* **2013**, *31* (24), 3915−3926.
(164) Jubin, D.; Dangel, R.; Meier, N.; Horst, F.; Lamprecht, T.; Weiss, J.; Beyeler, R.; Offrein, B. J.; Halter, M.; Stieger, R.; Betschon, F. Polymer Waveguide-Based Multilayer Optical Connector. *Proc. SPIE* **2010**, *7607*, 76070K.
(165) IPC. IPC TM-650 Test Methods Manual. https://www.ipc.org/test-methods.aspx (accessed April 22, 2020).

https://dx.doi.org/10.1021/acsphotonics.0c00983
ACS Photonics XXXX, XXX, XXX−XXX

(166) Xinyuan, D.; Wang, X.; Lin, X.; Ding, D.; Pan, D.; Chen, R. Highly Flexible Polymeric Optical Waveguide for Out-of-Plane Optical Interconnects. *Opt. Express* **2010**, *18* (15), 16227.
(167) Bosman, E.; Van Steenberge, G.; Van Hoe, B.; Missinne, J.; Vanfleteren, J.; Van Daele, P. Highly Reliable Flexible Active Optical Links. *IEEE Photonics Technol. Lett.* **2010**, *22* (5), 287−289.
(168) Dangel, R.; Hofrichter, J.; Horst, F.; Jubin, D.; La Porta, A.; Meier, N.; Soganci, I. M.; Weiss, J.; Offrein, B. J. Polymer Waveguides for Electro-Optical Integration in Data Centers and High-Performance Computers. *Opt. Express* **2015**, *23* (4), 4736.
(169) Nieweglowski, K.; Lorenz, L.; Lüngen, S.; Tiedje, T.; Wolter, K. J.; Bock, K. Optical Coupling with Flexible Polymer Waveguides for Chip-to-Chip Interconnects in Electronic Systems. *Microelectron. Reliab.* **2018**, *84*, 121−126.
(170) Flores, A.; Song, S.; Yang, J. J.; Liu, Z.; Wang, M. R. High-Speed Optical Interconnect Coupler Based on Soft Lithography Ribbons. *J. Lightwave Technol.* **2008**, *26* (13), 1956−1963.
(171) Barwicz, T.; Lichoulas, T. W.; Taira, Y.; Martin, Y.; Takenobu, S.; Janta-Polczynski, A.; Numata, H.; Kimbrell, E. L.; Nah, J. W.; Peng, B.; Childers, D.; Leidy, R.; Khater, M.; Kamlapurkar, S.; Cyr, E.; Engelmann, S.; Fortier, P.; Boyer, N. Automated, High-Throughput Photonic Packaging. *Opt. Fiber Technol.* **2018**, *44*, 24−35.
(172) Shalaginov, M. Y.; Campbell, S. D.; An, S.; Zhang, Y.; Ríos, C.; Whiting, E. B.; Wu, Y.; Kang, L.; Zheng, B.; Fowler, C.; Zhang, H.; Werner, D. H.; Hu, J.; Gu, T. Design for Quality: Reconfigurable Flat Optics Based on Active Metasurfaces. *Nanophotonics* **2020**, *9*, 3505.
(173) Lu, T.-W.; Wu, C.-C.; Wang, C.; Lee, P.-T. Compressible 1D Photonic Crystal Nanolasers with Wide Wavelength Tuning. *Opt. Lett.* **2017**, *42* (12), 2267.
(174) Wang, J.; Yin, Y.; Hao, Q.; Huang, S.; Saei Ghareh Naz, E.; Schmidt, O. G.; Ma, L. External Strain Enabled Post-Modification of Nanomembrane-Based Optical Microtube Cavities. *ACS Photonics* **2018**, *5* (5), 2060−2067.
(175) Hsu, K.-S; Chiu, T.-T.; Lee, P.-T.; Shih, M.-H. Wavelength Tuning by Bending a Flexible Photonic Crystal Laser. *J. Lightwave Technol.* **2013**, *31* (12), 1960−1964.
(176) Gutruf, P.; Zou, C.; Withayachumnankul, W.; Bhaskaran, M.; Sriram, S.; Fumeaux, C. Mechanically Tunable Dielectric Resonator Metasurfaces at Visible Frequencies. *ACS Nano* **2016**, *10* (1), 133−141.
(177) Pryce, I. M.; Aydin, K.; Kelaita, Y. A.; Briggs, R. M.; Atwater, H. A. Highly Strained Compliant Optical Metamaterials with Large Frequency Tunability. *Nano Lett.* **2010**, *10* (10), 4222−4227.
(178) Malek, S. C.; Ee, H. S.; Agarwal, R. Strain Multiplexed Metasurface Holograms on a Stretchable Substrate. *Nano Lett.* **2017**, *17* (6), 3641−3645.
(179) She, A.; Zhang, S.; Shian, S.; Clarke, D. R.; Capasso, F. Adaptive Metalenses with Simultaneous Electrical Control of Focal Length, Astigmatism, and Shift. *Sci. Adv.* **2018**, *4* (2), eaap9957.
(180) Zhu, L.; Kapraun, J.; Ferrara, J.; Chang-Hasnain, C. J. Flexible Photonic Metastructures for Tunable Coloration. *Optica* **2015**, *2* (3), 255.
(181) Shen, Y.; Rinnerbauer, V.; Wang, I.; Stelmakh, V.; Joannopoulos, J. D.; Soljačić, M. Structural Colors from Fano Resonances. *ACS Photonics* **2015**, *2* (1), 27−32.
(182) Tseng, M. L.; Yang, J.; Semmlinger, M.; Zhang, C.; Nordlander, P.; Halas, N. J. Two-Dimensional Active Tuning of an Aluminum Plasmonic Array for Full-Spectrum Response. *Nano Lett.* **2017**, *17* (10), 6034−6039.
(183) Shih, M. H.; Hsu, K. S.; Kunag, W.; Yang, Y. C.; Wang, Y. C.; Tsai, S. K.; Liu, Y. C.; Chang, Z. C.; Wu, M. C. Compact Optical Curvature Sensor with a Flexible Microdisk Laser on a Polymer Substrate. *Opt. Lett.* **2009**, *34* (18), 2733.
(184) Choi, J. H.; No, Y. S.; So, J. P.; Lee, J. M.; Kim, K. H.; Hwang, M. S.; Kwon, S. H.; Park, H. G. A High-Resolution Strain-Gauge Nanolaser. *Nat. Commun.* **2016**, *7* (1), 1−8.
(185) Michon, J.; Geiger, S.; Li, L.; Goncalves, C.; Lin, H.; Richardson, K.; Jia, X.; Hu, J. 3D Integrated Photonics Platform with Deterministic Geometry Control. *Photonics Res.* **2020**, *8* (2), 194.
(186) Raghunathan, V.; Ye, W. N.; Hu, J.; Izuhara, T.; Michel, J.; Kimerling, L. Athermal Operation of Silicon Waveguides: Spectral, Second Order and Footprint Dependencies. *Opt. Express* **2010**, *18* (17), 17631.
(187) Missinne, J.; Teigell Benéitez, N.; Lamberti, A.; Chiesura, G.; Luyckx, G.; Mattelin, M. A.; Van Paepegem, W.; Van Steenberge, G. Thin and Flexible Polymer Photonic Sensor Foils for Monitoring Composite Structures. *Adv. Eng. Mater.* **2018**, *20* (6), 1701127.
(188) Hofmann, M.; Xiao, Y.; Sherman, S.; Gleissner, U.; Schmidt, T.; Zappe, H. Asymmetric Mach−Zehnder Interferometers without an Interaction Window in Polymer Foils for Refractive Index Sensing. *Appl. Opt.* **2016**, *55* (5), 1124.
(189) Barrios, C. A. Rapid On-Site Formation of a Free-Standing Flexible Optical Link for Sensing Applications. *Sensors* **2016**, *16* (10), 1643.
(190) Wang, Y.; Huang, C. J.; Jonas, U.; Wei, T.; Dostalek, J.; Knoll, W. Biosensor Based on Hydrogel Optical Waveguide Spectroscopy. *Biosens. Bioelectron.* **2010**, *25* (7), 1663−1668.
(191) Westerveld, W. J.; Pozo, J.; Harmsma, P. J.; Schmits, R.; Tabak, E.; van den Dool, T. C.; Leinders, S. M.; van Dongen, K. W. A.; Urbach, H. P.; Yousefi, M. Characterization of a Photonic Strain Sensor in Silicon-on-Insulator Technology. *Opt. Lett.* **2012**, *37* (4), 479−481.
(192) De Brabander, G. N.; Boyd, J. T.; Beheim, G. Integrated Optical Ring Resonator With Micromechanical Diaphragm for Pressure Sensing. *IEEE Photonics Technol. Lett.* **1994**, *6* (5), 671−673.
(193) Aieta, F.; Genevet, P.; Kats, M.; Capasso, F. Aberrations of Flat Lenses and Aplanatic Metasurfaces. *Opt. Express* **2013**, *21* (25), 31530.
(194) Chen, M.; Kim, M.; Wong, A. M. H.; Eleftheriades, G. V. Huygens' Metasurfaces from Microwaves to Optics: A Review. *Nanophotonics* **2018**, *7* (6), 1207−1231.
(195) Dietrich, P.-I.; Blaicher, M.; Reuter, I.; Billah, M.; Hoose, T.; Hofmann, A.; Caer, C.; Dangel, R.; Offrein, B.; Troppenz, U.; Moehrle, M.; Freude, W.; Koos, C. In Situ 3D Nanoprinting of Free-Form Coupling Elements for Hybrid Photonic Integration. *Nat. Photonics* **2018**, *12* (4), 241−247.
(196) Yu, S.; Zuo, H.; Wang, X.; Sun, X.; Liu, J.; Hu, J.; Gu, T. Seamless Hybrid-Integrated Interconnect NEtwork (SHINE). *2019 Optical Fiber Communications Conference and Exhibition, OFC 2019 - Proceedings* **2019**, M4D.5.
(197) Yu, S.; Zuo, H.; Sun, X.; Liu, J.; Gu, T.; Hu, J. Optical Free-Form Couplers for High-Density Integrated Photonics (OFFCHIP): A Universal Optical Interface. *J. Lightwave Technol.* **2020**, *38*, 3358.
(198) Ohrt, C.; Acar, Y.; Seidel, A.; Cheng, W.; Kiyan, R.; Chichkov, B. N. Fidelity of Soft Nano-Imprint Lithographic Replication of Polymer Masters Fabricated by Two-Photon Polymerization. *Int. J. Adv. Manuf. Technol.* **2012**, *63* (1−4), 103−108.
(199) Pashaie, R.; Anikeeva, P.; Lee, J. H.; Prakash, R.; Yizhar, O.; Prigge, M.; Chander, D.; Richner, T. J.; Williams, J. Optogenetic Brain Interfaces. *IEEE Rev. Biomed. Eng.* **2014**, *7*, 3−30.
(200) Alt, M. T.; Fiedler, E.; Rudmann, L.; Ordonez, J. S.; Ruther, P.; Stieglitz, T. Let There Be Light-Optoprobes for Neural Implants. *Proc. IEEE* **2017**, *105* (1), 101−138.
(201) Son, Y.; Jenny Lee, H.; Kim, J.; Shin, H.; Choi, N.; Justin Lee, C.; Yoon, E. S.; Yoon, E.; Wise, K. D.; Geun Kim, T.; Cho, I. J. In Vivo Optical Modulation of Neural Signals Using Monolithically Integrated Two-Dimensional Neural Probe Arrays. *Sci. Rep.* **2015**, *5* (1), 1−11.
(202) McAlinden, N.; Gu, E.; Dawson, M. D.; Sakata, S.; Mathieson, K. Optogenetic Activation of Neocortical Neurons in Vivo with a Sapphire-Based Micro-Scale LED Probe. *Front. Neural Circuits* **2015**, *9* (May), 25.
(203) Li, B.; Lee, K.; Masmanidis, S. C.; Li, M. A Nanofabricated Optoelectronic Probe for Manipulating and Recording Neural Dynamics. *J. Neural Eng.* **2018**, *15* (4), 046008.
(204) Poddubny, A.; Iorsh, I.; Belov, P.; Kivshar, Y. Hyperbolic Metamaterials. *Nat. Photonics* **2013**, *7* (12), 948−957.

https://dx.doi.org/10.1021/acsphotonics.0c00983
ACS Photonics XXXX, XXX, XXX−XXX

(205) Drachev, V. P.; Podolskiy, V. A.; Kildishev, A. V. Hyperbolic Metamaterials: New Physics behind a Classical Problem. *Opt. Express* **2013**, *21* (12), 15048.
(206) Lu, L.; Simpson, R. E.; Valiyaveedu, S. K. Active Hyperbolic Metamaterials: Progress, Materials and Design. *J. Opt.* **2018**, *20* (10), 103001.
(207) Boltasseva, A.; Atwater, H. A. Low-Loss Plasmonic Metamaterials. *Science (Washington, DC, U. S.)* **2011**, *331* (6015), 290−291.
(208) Kinsey, N.; DeVault, C.; Boltasseva, A.; Shalaev, V. M. Near-Zero-Index Materials for Photonics. *Nat. Rev. Mater.* **2019**, *4* (12), 742−760.
(209) Niu, X.; Hu, X.; Chu, S.; Gong, Q. Epsilon-Near-Zero Photonics: A New Platform for Integrated Devices. *Adv. Opt. Mater.* **2018**, *6* (10), 1701292.
(210) Riley, C. T.; Smalley, J. S. T.; Brodie, J. R. J.; Fainman, Y.; Sirbuly, D. J.; Liu, Z. Near-Perfect Broadband Absorption from Hyperbolic Metamaterial Nanoparticles. *Proc. Natl. Acad. Sci. U. S. A.* **2017**, *114* (6), 1264−1268.
(211) Naik, G. V.; Kim, J.; Boltasseva, A. Oxides and Nitrides as Alternative Plasmonic Materials in the Optical Range [Invited]. *Opt. Mater. Express* **2011**, *1* (6), 1090.
(212) Naik, G. V.; Shalaev, V. M.; Boltasseva, A. Alternative Plasmonic Materials: Beyond Gold and Silver. *Adv. Mater.* **2013**, *25*, 3264−3294.
(213) Liberal, I.; Mahmoud, A. M.; Engheta, N. Geometry-Invariant Resonant Cavities. *Nat. Commun.* **2016**, *7* (1), 1−7.
(214) Lindenmann, N.; Balthasar, G.; Hillerkuss, D.; Schmogrow, R.; Jordan, M.; Leuthold, J.; Freude, W.; Koos, C. Photonic Wire Bonding: A Novel Concept for Chip-Scale Interconnects. *Opt. Express* **2012**, *20* (16), 17667.
(215) Kim, B. H.; Liu, F.; Yu, Y.; Jang, H.; Xie, Z.; Li, K.; Lee, J.; Jeong, J. Y.; Ryu, A.; Lee, Y.; Kim, D. H.; Wang, X.; Lee, K. H.; Lee, J. Y.; Won, S. M.; Oh, N.; Kim, J.; Kim, J. Y.; Jeong, S. J.; Jang, K. I.; Lee, S.; Huang, Y.; Zhang, Y.; Rogers, J. A. Mechanically Guided Post-Assembly of 3D Electronic Systems. *Adv. Funct. Mater.* **2018**, *28* (48), 1803149.
(216) Cho, J. H.; Gracias, D. H. Self-Assembly of Lithographically Patterned Nanoparticles. *Nano Lett.* **2009**, *9* (12), 4049−4052.
(217) Wang, H.; Sun, P.; Yin, L.; Sheng, X. 3D Electronic and Photonic Structures as Active Biological Interfaces. *InfoMat* **2020**, *2* (3), 527−552.
(218) Arpin, K. A.; Mihi, A.; Johnson, H. T.; Baca, A. J.; Rogers, J. A.; Lewis, J. A.; Braun, P. V. Multidimensional Architectures for Functional Optical Devices. *Adv. Mater.* **2010**, *22*, 1084−1101.
(219) Suzuki, K.; Kitano, K.; Ishizaki, K.; Noda, S. Three-Dimensional Photonic Crystals Created by Single-Step Multi-Directional Plasma Etching. *Opt. Express* **2014**, *22* (14), 17099−17106.
(220) Zhang, Y.; Zhang, F.; Yan, Z.; Ma, Q.; Li, X.; Huang, Y.; Rogers, J. A. Printing, Folding and Assembly Methods for Forming 3D Mesostructures in Advanced Materials. *Nat. Rev. Mater.* **2017**, *2* (4), 1−17.
(221) van Manen, T.; Janbaz, S.; Zadpoor, A. A. Programming the Shape-Shifting of Flat Soft Matter. *Mater. Today* **2018**, *21* (2), 144−163.
(222) Cheng, X.; Zhang, Y. Micro/Nanoscale 3D Assembly by Rolling, Folding, Curving, and Buckling Approaches. *Adv. Mater.* **2019**, *31* (36), 1901895.
(223) Liu, Z.; Cui, A.; Li, J.; Gu, C. Folding 2D Structures into 3D Configurations at the Micro/Nanoscale: Principles, Techniques, and Applications. *Adv. Mater.* **2019**, *31* (4), 1802211.
(224) Yan, Z.; Zhang, F.; Wang, J.; Liu, F.; Guo, X.; Nan, K.; Lin, Q.; Gao, M.; Xiao, D.; Shi, Y.; Qiu, Y.; Luan, H.; Kim, J. H.; Wang, Y.; Luo, H.; Han, M.; Huang, Y.; Zhang, Y.; Rogers, J. A. Controlled Mechanical Buckling for Origami-Inspired Construction of 3D Microstructures in Advanced Materials. *Adv. Funct. Mater.* **2016**, *26* (16), 2629−2639.
(225) Xu, Z.; Fan, Z.; Zi, Y.; Zhang, Y.; Huang, Y. An Inverse Design Method of Buckling-Guided Assembly for Ribbon-Type 3D Structures. *J. Appl. Mech.* **2020**, *87* (3), 031004.
(226) Fan, Z.; Yang, Y.; Zhang, F.; Xu, Z.; Zhao, H.; Wang, T.; Song, H.; Huang, Y.; Rogers, J. A.; Zhang, Y. Inverse Design Strategies for 3D Surfaces Formed by Mechanically Guided Assembly. *Adv. Mater.* **2020**, *32* (14), 1908424.
(227) Guo, X.; Xu, Z.; Zhang, F.; Wang, X.; Zi, Y.; Rogers, J. A.; Huang, Y.; Zhang, Y. Reprogrammable 3D Mesostructures Through Compressive Buckling of Thin Films with Prestrained Shape Memory Polymer. *Acta Mech. Solida Sin.* **2018**, *31* (5), 589−598.
(228) Park, J. K.; Nan, K.; Luan, H.; Zheng, N.; Zhao, S.; Zhang, H.; Cheng, X.; Wang, H.; Li, K.; Xie, T.; Huang, Y.; Zhang, Y.; Kim, S.; Rogers, J. A. Remotely Triggered Assembly of 3D Mesostructures Through Shape-Memory Effects. *Adv. Mater.* **2019**, *31* (52), 1905715.
(229) Park, Y.; Luan, H.; Kwon, K.; Zhao, S.; Franklin, D.; Wang, H.; Zhao, H.; Bai, W.; Kim, J. U.; Lu, W.; Kim, J. H.; Huang, Y.; Zhang, Y.; Rogers, J. A. Transformable, Freestanding 3D Mesostructures Based on Transient Materials and Mechanical Interlocking. *Adv. Funct. Mater.* **2019**, *29* (40), 1903181.
(230) Leong, T. G.; Randall, C. L.; Benson, B. R.; Bassik, N.; Stern, G. M.; Gracias, D. H. Tetherless Thermobiochemically Actuated Microgrippers. *Proc. Natl. Acad. Sci. U. S. A.* **2009**, *106* (3), 703−708.
(231) Cho, J. H.; Azam, A.; Gracias, D. H. Three Dimensional Nanofabrication Using Surface Forces. *Langmuir* **2010**, *26* (21), 16534−16539.
(232) Cho, J. H.; Keung, M. D.; Verellen, N.; Lagae, L.; Moshchalkov, V. V.; Van Dorpe, P.; Gracias, D. H. Nanoscale Origami for 3D Optics. *Small* **2011**, *7* (14), 1943−1948.
(233) Buljac, A.; Jailin, C.; Mendoza, A.; Neggers, J.; Taillandier-Thomas, T.; Bouterf, A.; Smaniotto, B.; Hild, F.; Roux, S. Digital Volume Correlation: Review of Progress and Challenges. *Exp. Mech.* **2018**, *58* (5), 661−708.
(234) Franck, C.; Hong, S.; Maskarinec, S. A.; Tirrell, D. A.; Ravichandran, G. Three-Dimensional Full-Field Measurements of Large Deformations in Soft Materials Using Confocal Microscopy and Digital Volume Correlation. *Exp. Mech.* **2007**, *47* (3), 427−438.
(235) Toyjanova, J.; Bar-Kochba, E.; López-Fagundo, C.; Reichner, J.; Hoffman-Kim, D.; Franck, C. High Resolution, Large Deformation 3D Traction Force Microscopy. *PLoS One* **2014**, *9* (4), e90976.
(236) Style, R. W.; Boltyanskiy, R.; German, G. K.; Hyland, C.; Macminn, C. W.; Mertz, A. F.; Wilen, L. A.; Xu, Y.; Dufresne, E. R. Traction Force Microscopy in Physics and Biology. *Soft Matter* **2014**, *10*, 4047−4055.
(237) Webb, R. H. Confocal Optical Microscopy. *Rep. Prog. Phys.* **1996**, *59* (3), 427−471.
(238) Polacheck, W. J.; Chen, C. S. Measuring Cell-Generated Forces: A Guide to the Available Tools. *Nat. Methods* **2016**, *13*, 415−423.
(239) Ribeiro, A. J. S.; Denisin, A. K.; Wilson, R. E.; Pruitt, B. L. For Whom the Cells Pull: Hydrogel and Micropost Devices for Measuring Traction Forces. *Methods* **2016**, *94*, 51−64.
(240) Maskarinec, S. A.; Franck, C.; Tirrell, D. A.; Ravichandran, G. Quantifying Cellular Traction Forces in Three Dimensions. *Proc. Natl. Acad. Sci. U. S. A.* **2009**, *106* (52), 22108−22113.

https://dx.doi.org/10.1021/acsphotonics.0c00983
ACS Photonics XXXX, XXX, XXX−XXX